Title

CYP5122A1 encodes an essential sterol C4-methyl oxidase in *Leishmania donovani* and determines the antileishmanial activity of antifungal azoles

Supplementary Figures and Tables:

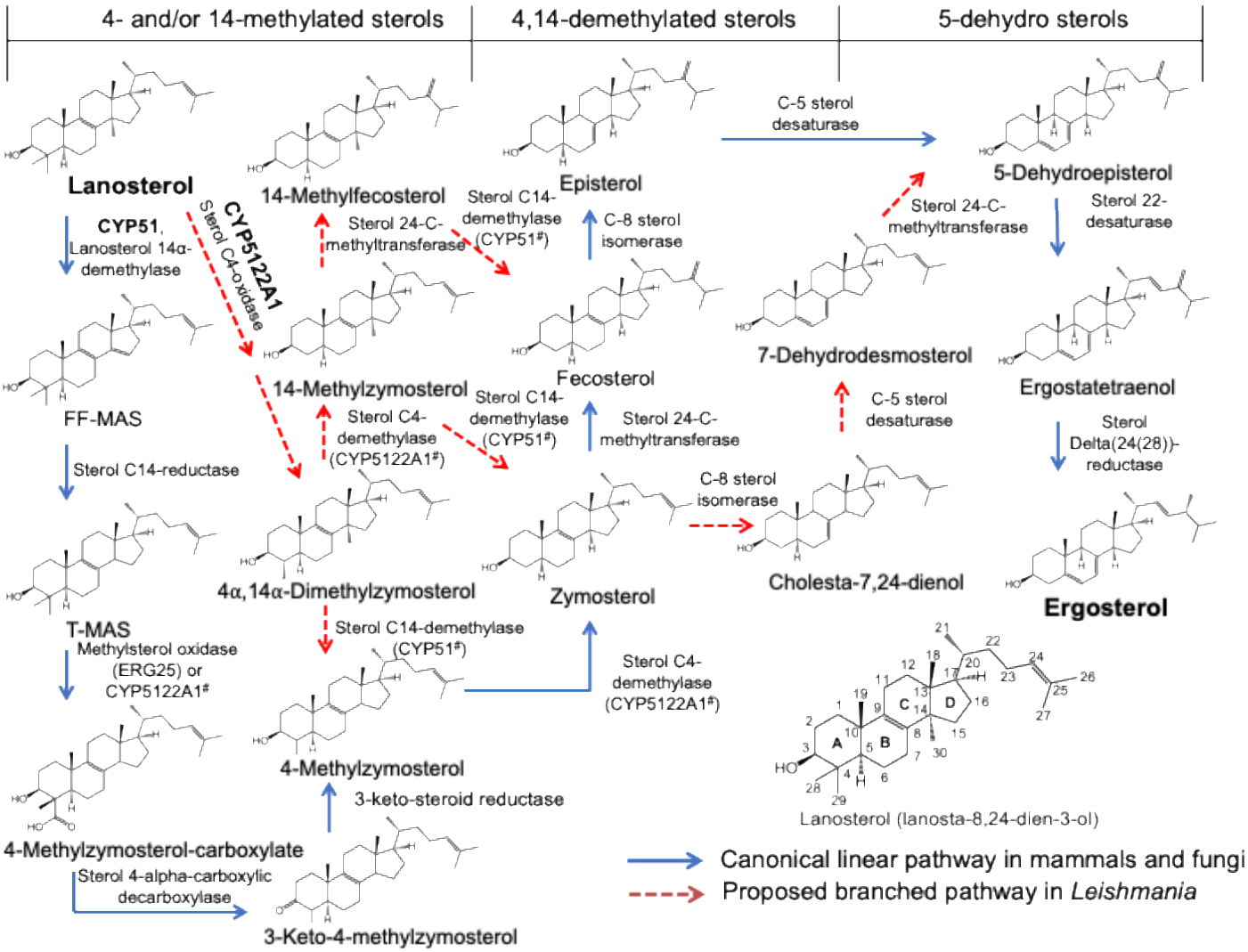

Supplementary Fig. 1. Proposed branched ergosterol biosynthesis pathway in *Leishmania* with CYP5122A1 serving as a sterol C4 methyl-oxidase, which is adapted from the previously proposed pathway by Feng *et al*. in 2022 [ref. 18]. # CYP51 and CYP5122A1 are presumed to be the sterol C14- and C4-demethylase in these downstream reactions, respectively.

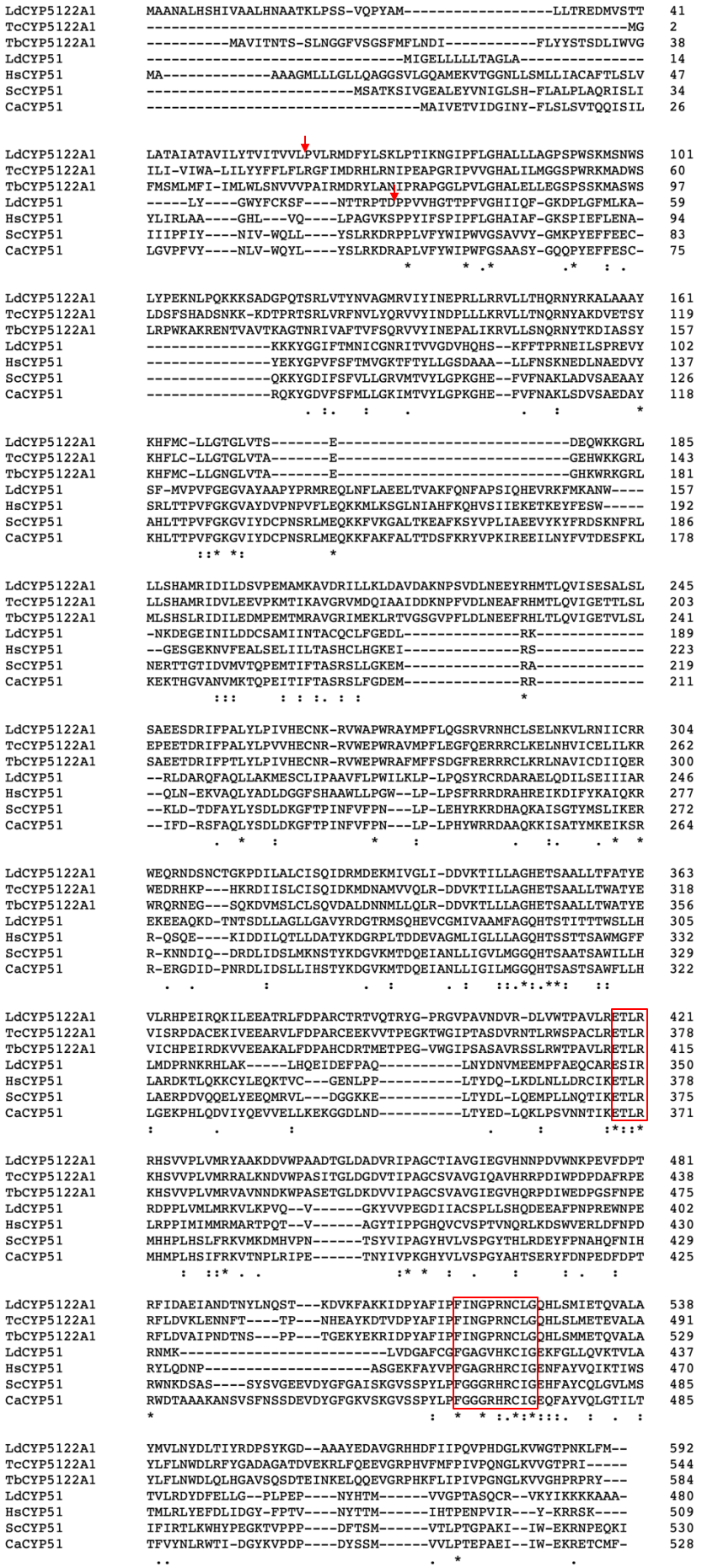
LdCYP5122A1 MAANALHSHIVAALHNAATKLPSS-VQPYAM----------LLTREDMVSTT 41
TcCYP5122A1 ----------MG 2
TbCYP5122A1 ----------MAVITNTS-SLNGGFVSGSFMFLNDI----------FLYYSTSDLIWVG 38
LdCYP51 ----------MIGELLLLLTAGLA---------- 14
HsCYP51 MA----------AAAGMLLLGLLQAGGSVLGQAMEKVTGGNLLSMLLIACAFTLSLV 47
ScCYP51 ----------MSATKSIVGEALEYVNIGLSH-FLALPLAQRISLI 34
CaCYP51 ----------MAIVETVIDGINY-FLSLSVTQQISIL 26
LdCYP5122A1 LATAIATAVILYTVITVVLPVLRMDFYLSKLPTIKNGIPFLGHALLLAGPSPWSKMSNWS 101
TcCYP5122A1 ILI-VIWA-LILYYFFLFLRGFIMDRHLRNIPEAPGRIPVVGHALILMGGSPWRKMADWS 60
TbCYP5122A1 FMSMLMFI-IMLWLSNVVVPAIRMDRYLANIPRAPGGLPVLGHALELLEGSPSSKMASWS 97
LdCYP51 -----LY----GWYFCKSF----NTTRPTDPPVVHGTTPFVGHIIQF-GKDPLGFMLKA- 59
HsCYP51 YLIRLAA----GHL---VQ----LPAGVKSPPYIFSPIPFLGHAIAF-GKSPIEFLENA- 94
ScCYP51 IIIPFIY----NIV-WQLL----YSLRKDRPPLVFYWIPWVGSAVVY-GMKPYEFFEEC- 83
CaCYP51 LGVPFVY----NLV-WQYL----YSLRKDRAPLVFYWIPWFGSAASY-GQQPYEFFESC- 75
LdCYP5122A1 LYPEKNLPQKKKSADGPQTSRLVTYNVAGMRVIYINEPRLLRRVLLTHQRNYRKALAAAY 161
TcCYP5122A1 LDSFSHADSNKK-KDTPRTSRLVRFNVLYQRVVYINDPLLLKRVLLTNQRNYAKDVETSY 119
TbCYP5122A1 LRPWKAKRENTVAVTKAGTNRIVAFTVFSQRVVYINEPALIKRVLLSNQRNYTKDIASSY 157
LdCYP51 ----------KKKYGGIFTMNICGNRITVVGDVHQHS--KFFTPRNEILSPREVY 102
HsCYP51 ----------YEKYGPVFSFTMVGKTFTYLLGSDAAA--LLFNSKNEDLNAEDVY 137
ScCYP51 ----------QKKYGDIFSFVLLGRVMTVYLGPKGHE--FVFNAKLADVSAEAAY 126
CaCYP51 ----------RQKYGDVFSFMLLGKIMTVYLGPKGHE--FVFNAKLSDVSAEDAY 118
LdCYP5122A1 KHFMC-LLGTGLVTS-------E----------DEQWKKGRL 185
TcCYP5122A1 KHFLC-LLGTGLVTA-------E----------GEHWKKGRL 143
TbCYP5122A1 KHFMC-LLGNGLVTA-------E----------GHKWRKGRL 181
LdCYP51 SF-MVPVFGEGVAYAAPYPRMREQLNFLAEELTVAKFQNFAPSIQHEVRKFMKANW---- 157
HsCYP51 SRLTTPVFGKGVAYDVPNPVFLEQKKMLKSGLNIAHFKQHVSIIEKETKEYFESW----- 192
ScCYP51 AHLTTPVFGKGVIYDCPNSRLMEQKKFVKGALTKEAFKSYVPLIAEEVYKYFRDSKNFRL 186
CaCYP51 KHLTTPVFGKGVIYDCPNSRLMEQKKFAKFALTTDSFKRYVPKIREEILNYFVTDESFKL 178
LdCYP5122A1 LLSHAMRIDILDSVPEMAMKAVDRILLKLDAVDAKNPSVDLNEEYRHMTLQVISESALSL 245
TcCYP5122A1 LLSHAMRIDVLEEVPKMTIKAVGRVMDQIAAIDDKNPFVDLNEAFRHMTLQVIGETTLSL 203
TbCYP5122A1 MLSHSLRIDILEDMPEMTMRAVGRIMEKLRTVGSGVPFLDLNEEFRHLTLQVIGETVLSL 241
LdCYP51 -NKDEGEINILDDCSAMIINTACQCLFGEDL----------RK---------- 189
HsCYP51 --GESGEKNVFEALSELIILTASHCLHGKEI----------RS---------- 223
ScCYP51 NERTTGTIDVMVTQPEMTIFTASRSLLGKEM----------RA---------- 219
CaCYP51 KEKTHGVANVMKTQPEITIFTASRSLFGDEM----------RR---------- 211
LdCYP5122A1 SAEESDRIFPALYLPIVHECNK-RVWAPWRAYMPFLQGSRVRNHCLSELNKVLRNIICRR 304
TcCYP5122A1 EPEETDRIFPALYLPVVHECNR-RVWEPWRAVMPFLEGFQERRRCLKELNHVICELILKR 262
TbCYP5122A1 SAEETDRIFPTLYLPIVHECNR-RVWEPWRAFMFFSDGFRERRRCLKRLNAVICDIIQER 300
LdCYP51 --RLDARQFAQLLAKMESCLIPAAVFLPWILKLP-LPQSYRCRDARAELQDILSEIIIAR 246
HsCYP51 --QLN-EKVAQLYADLDGGFSHAAWLLPGW--LP-LPSFRRRDRAHREIKDIFYKAIQKR 277
ScCYP51 --KLD-TDFAYLYSDLDKGFTPINFVFPN---LP-LEHYRKRDHAQKAISGTYMSLIKER 272
CaCYP51 --IFD-RSFAQLYSDLDKGFTPINFVFPN---LP-LPHYWRRDAAQKKISATYMKEIKSR 264
LdCYP5122A1 WEQRNDSNCTGKPDILALCISQIDRMDEKMIVGLI-DDVKTILLAGHETSAALLTFATYE 363
TcCYP5122A1 WEDRHKP---HKRDIISLCISQIDKMDNAMVVQLR-DDVKTILLAGHETSAALLTWATYE 318
TbCYP5122A1 WRQRNEG---SQKDVMSLCLSQVDALDNNMLLQLR-DDVKTLLLAGHETSAALLTWATYE 356
LdCYP51 EKEEAQKD-TNTSDLLAGLLGAVYRDGTRMSQHEVCGMIVAAMFAGQHTSTITTTWSLLH 305
HsCYP51 R-QSQE----KIDDILQTLLDATYKDGRPLTDDEVAGMLIGLLLAGQHTSSTTSAWMGFF 332
ScCYP51 R-KNNDIQ--DRDLIDSLMKNSTYKDGVKMTDQEIANLLIGVLMGGQHTSAATSAWILLH 329
CaCYP51 R-ERGDID-PNRDLIDSLLIHSTYKDGVKMTDQEIANLLIGILMGGQHTSASTSAWFLLH 322
LdCYP5122A1 VLRHPEIRQKILEEATRLFDPARCTRTVQTRYG-PRGVPAVNDVR-DLVWTPAVLRETLR 421
TcCYP5122A1 VISRPDACEKIVEEARVLFDPARCEEKVVTPEGKTWGIPTASDVRNTLRWSPACLRETLR 378
TbCYP5122A1 VICHPEIRDKVVEEAKALFDPAHCDRTMETPEG-VWGIPSASAVRSSLRWTPAVLRETLR 415
LdCYP51 LMDPRNKRHLAK-----LHQEIDEFPAQ----------LNYDNVMEEMPFAEQCARESIR 350
HsCYP51 LARDKTLQKKCYLEQKTVC---GENLPP----------LTYDQ-LKDLNLLDRCIKETLR 378
ScCYP51 LAERPDVQQELYEEQMRVL---DGGKKE----------LTYDL-LQEMPLLNQTIKETLR 375
CaCYP51 LGEKPHLQDVIYQEVVELLKEKGGDLND----------LTYED-LQKLPSVNNTIKETLR 371
LdCYP5122A1 RHSVVPLVMRYAAKDDVWPAADTGLDADVRIPAGCTIAVGIEGVHNNPDVWNKPEVFDPT 481
TcCYP5122A1 KHSVVPLVMRRALKNDVWPASITGLDGDVTIPAGCSVAVGIQAVHRRPDIWPDPDAFRPE 438
TbCYP5122A1 KHSVVPLVMRVAVNNDKWPASETGLDKDVVIPAGCSVAVGIEGVHQRPDIWEDPGSFNPE 475
LdCYP51 RDPPLVMLMRKVLKPVQ--V------GKYVVPEGDIIACSPLLSHQDEEAFPNPREWNPE 402
HsCYP51 LRPPIMIMMRMARTPQT--V------AGYTIPPGHQVCVSPTVNQRLKDSWVERLDFNPD 430
ScCYP51 MHHPLHSLFRKVMKDMHVPN------TSYVIPAGYHVLVSPGYTHLRDEYFPNAHQFNIH 429
CaCYP51 MHMPLHSIFRKVTNPLRIPE------TNYIVPKGHYVLVSPGYAHTSERYFDNPEDFDPT 425
LdCYP5122A1 RFIDAEIANDTNYLNQST---KDVKFAKKIDPYAFIPFINGPRNCLGQHLSMIETQVALA 538
TcCYP5122A1 RFLDVKLENNFT----TP---NHEAYKDTVDPYAFIPFINGPRNCLGQHLSLMETEVALA 491
TbCYP5122A1 RFLDVAIPNDTNS---PP---TGEKYEKRIDPYAFIPFINGPRNCLGQHLSMMETQVALA 529
LdCYP51 RNMK----------LVDGAFCGFGAGVHKCIGEKFGLLQVKTVLA 437
HsCYP51 RYLQDNP----------ASGEKFAYVPFGAGRHRCIGENFAYVQIKTIWS 470
ScCYP51 RWNKDSAS----SYSVGEEVDYGFGAISKGVSSPYLPFGGGRHRCIGEHFAYCQLGVLMS 485
CaCYP51 RWDTAAAKANSVSFNSSDEVDYGFGKVSKGVSSPYLPFGGGRHRCIGEQFAYVQLGTILT 485
LdCYP5122A1 YMVLNYDLTIYRDPSYKGD--AAAYEDAVGRHHDFIIPQVPHDGLKVWGTPNKLFM-- 592
TcCYP5122A1 YLFLNWDLRFYGADAGATDVEKRLFQEEVGRPHVFMFPIVPQNGLKVVGTPRI----- 544
TbCYP5122A1 YLFLNWDLQLHGAVSQSDTEINKELQQEVGRPHKFLIPIVPGNGLKVVGHPRPRY--- 584
LdCYP51 TVLRDYDFELLG--PLPEP----NYHTM------VVGPTASQCR--VKYIKKKKAAA- 480
HsCYP51 TMLRLYEFDLIDGY-FPTV----NYTTM------IHTPENPVIR---Y-KRRSK---- 509
ScCYP51 IFIRTLKWHYPEGKTVPPP----DFTSM------VTLPTGPAKI--IW-EKRNPEQKI 530
CaCYP51 TFVYNLRWTI-DGYKVPDP----DYSSM------VVLPTEPAEI--IW-EKRETCMF- 528

Supplementary Fig. 2. Multiple sequence alignment of CYP5122A1 and CYP51 enzymes using Clustal Omega (available at https://www.ebi.ac.uk/Tools/msa/clustalo/). The highly conserved EXXR motif and the P450 signature motif FXXGX(H/R)XCXG are boxed. The sites of truncation are indicated by arrows. LdCYP5122A1: *L. donovani* CYP5122A1 (XP_003861867.1); TcCYP5122A1: *T. cruzi* CYP5122A1 (XP_807973.1); TbCYP5122A1: *T. brucei* CYP5122A1 (XP_843664.1); LdCYP51: *L. donovani* CYP51 (XP_003859085.1); HsCYP51: *Homo sapiens* CYP51 (NP_000777.1); ScCYP51: *Saccharomyces cerevisiae* CYP51 (NP_011871.1); CaCYP51: *Candida albicans* CYP51 (XP_716761.1).

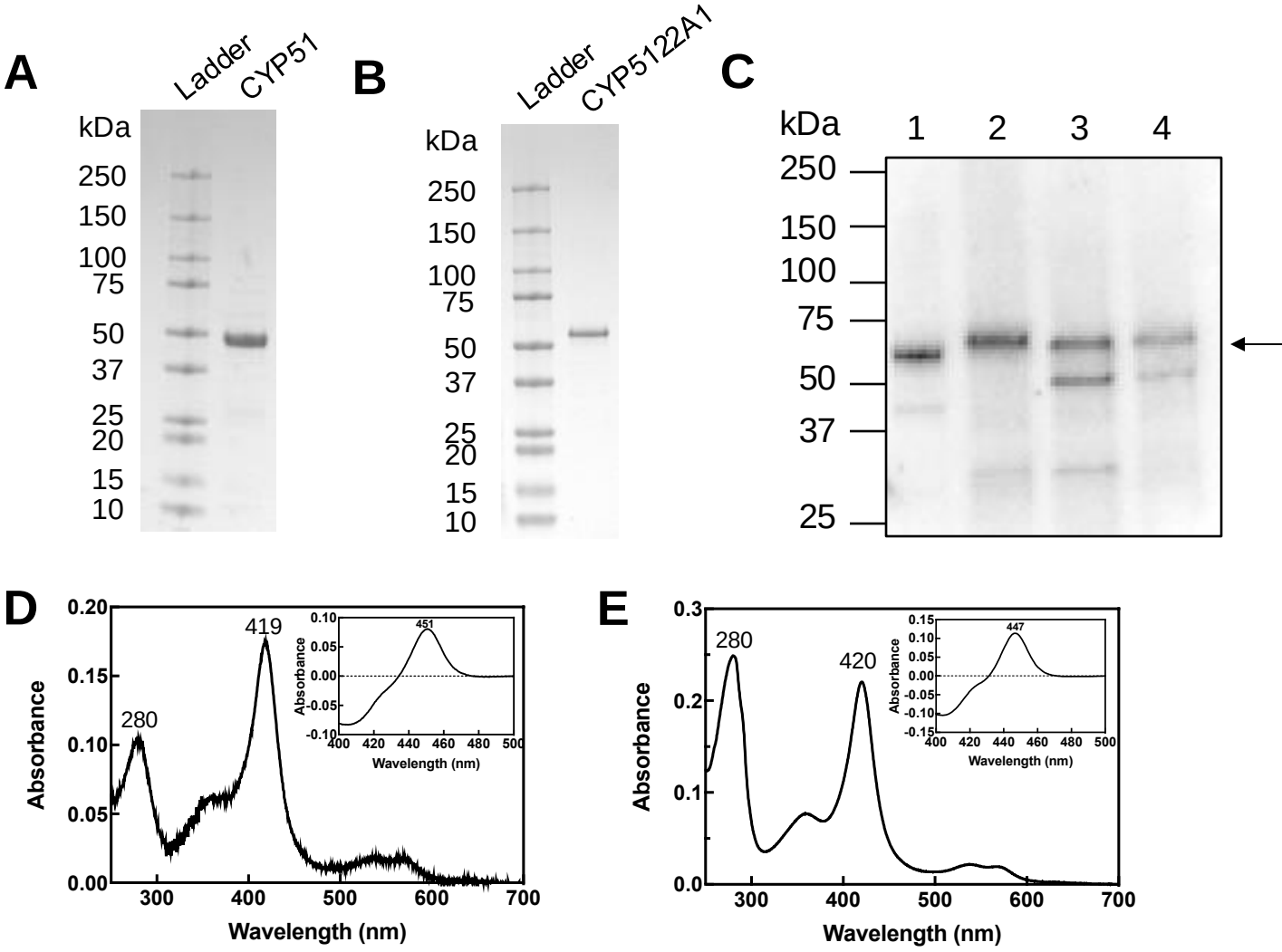

Supplementary Fig. 3. Purified CYP51 and CYP5122A1 exhibited characteristic spectral properties and CYP5122A1 was detected in various *Leishmania* parasites.
(A-B) SDS-PAGE analysis of recombinant CYP51 and CYP5122A1. This purification was repeated at least half a dozen times for each CYP with the same results. (C) Detection of CYP5122A1 by Western blot analysis in Lane 1, recombinant *L. donovani* CYP5122A1 (62 kDa). Lane 2, *L. major* (LV39 strain) cell lysates (68 kDa). Lane 3, *L donovani* (LV82 strain) cell lysates (66 kDa). Lane 4, *L donovani (*Ld1S strain) cell lysates. The absolute absorbance spectra were measured for recombinant CYP51 (D and CYP5122A1 (E), showing the Soret band at around 420 nm. The insets show the CO difference spectra of sodium dithionite-reduced CYPs which exhibited the characteristic peak at around 450 nm.

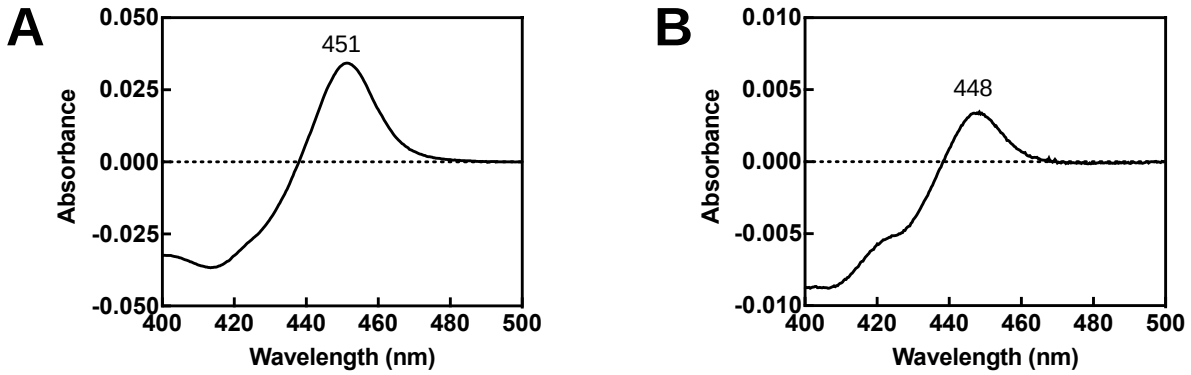

Supplementary Fig. 4. Reduced CO difference spectra of TbCPR-reduced CYPs in the presence of NADPH. (A) CYP51 and (B) CYP5122A1 exhibited the characteristic P450 peak.

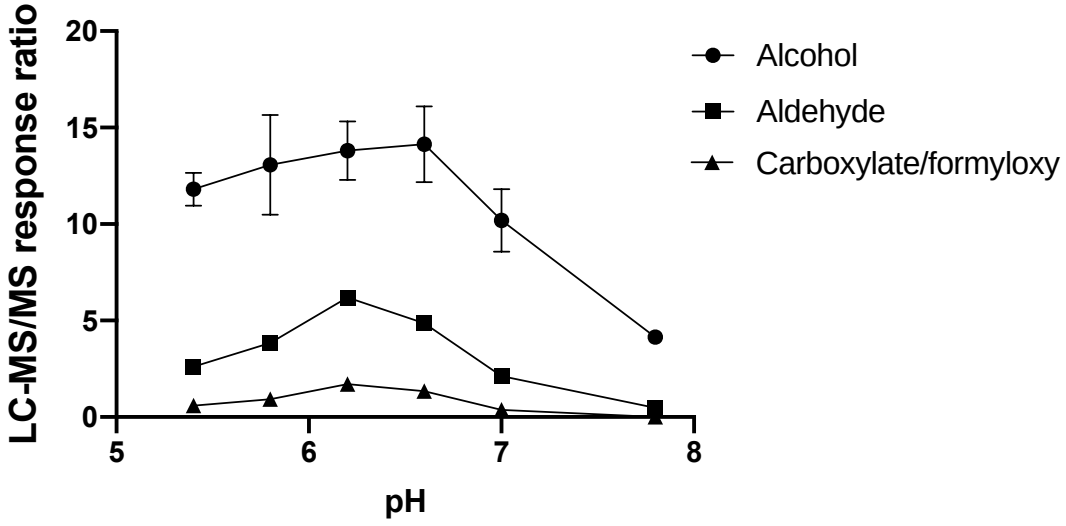

Supplementary Fig. 5. pH dependence of CYP5122A1-catalyzed oxidation of lanosterol. Symbols and error bars represent the means and standard deviations of triplicate determinations. Source data are provided as a Source Data file.

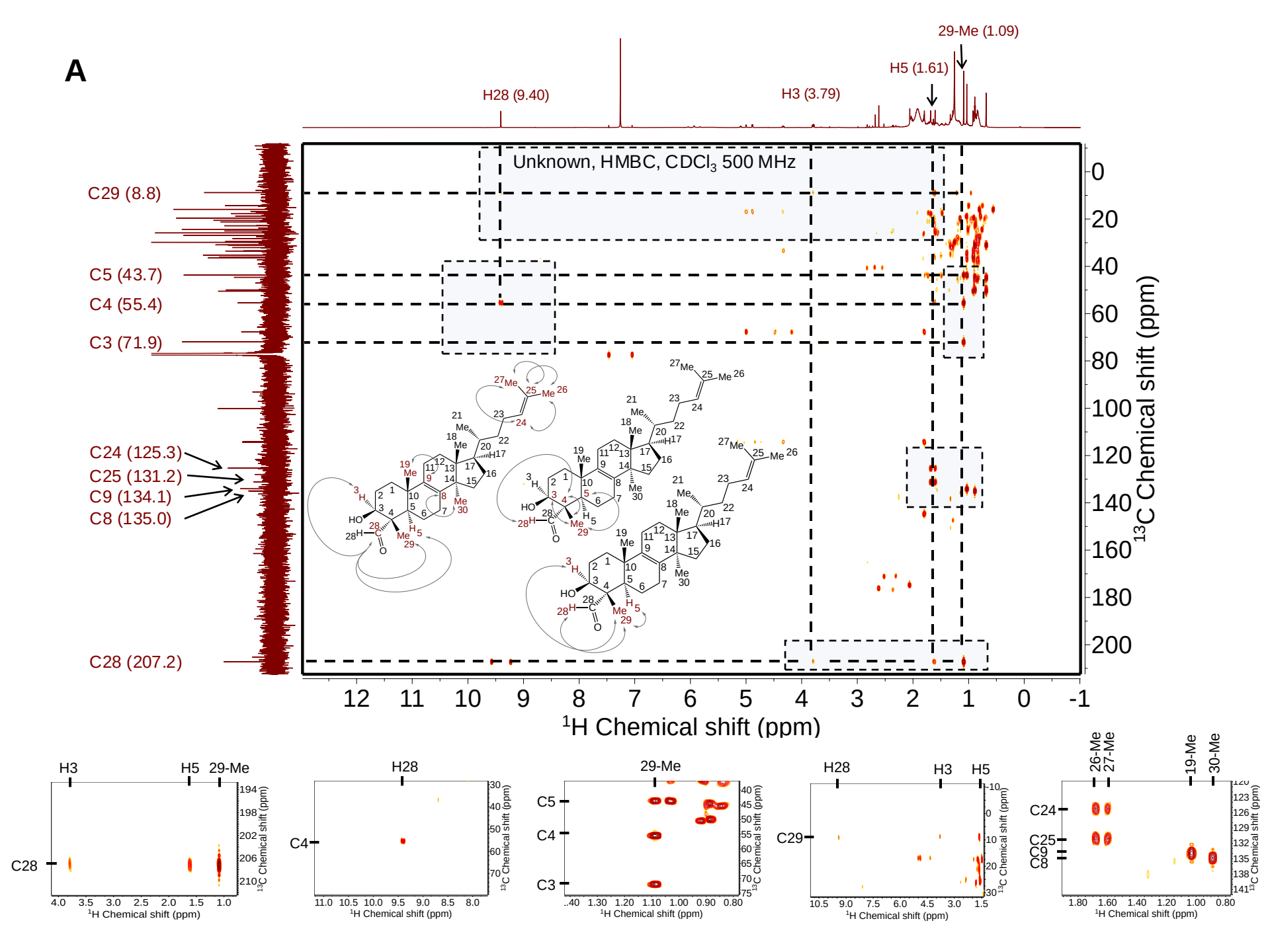
A
29-Me (1.09)
H5 (1.61)
H28 (9.40)
H3 (3.79)
Unknown, HMBC, CDCl3 500 MHz
C29 (8.8)
C5 (43.7)
C4 (55.4)
C3 (71.9)
C24 (125.3)
C25 (131.2)
C9 (134.1)
C8 (135.0)
C28 (207.2)
13C Chemical shift (ppm)
1H Chemical shift (ppm)
H3
H5
29-Me
H28
C28
C4
C5
C3
C29
26-Me
27-Me
19-Me
30-Me
C24
C25
C9
C8

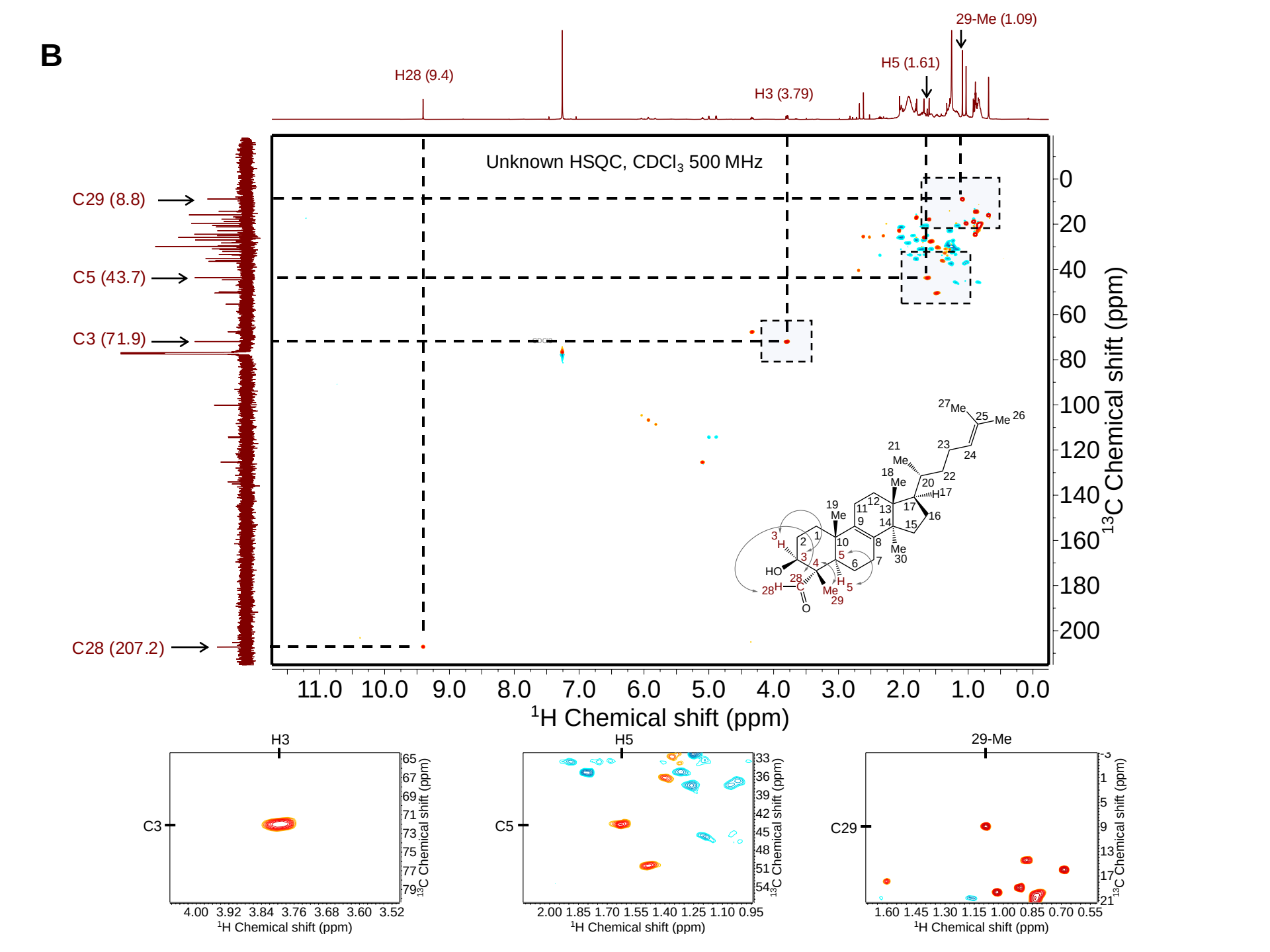
B
H28 (9.4)
H3 (3.79)
H5 (1.61)
29-Me (1.09)
Unknown HSQC, CDCl3 500 MHz
C29 (8.8)
C5 (43.7)
C3 (71.9)
C28 (207.2)
11.0 10.0 9.0 8.0 7.0 6.0 5.0 4.0 3.0 2.0 1.0 0.0
1H Chemical shift (ppm)
0 20 40 60 80 100 120 140 160 180 200
13C Chemical shift (ppm)
H3
C3
4.00 3.92 3.84 3.76 3.68 3.60 3.52
1H Chemical shift (ppm)
65 67 69 71 73 75 77 79
13C Chemical shift (ppm)
H5
C5
2.00 1.85 1.70 1.55 1.40 1.25 1.10 0.95
1H Chemical shift (ppm)
33 36 39 42 45 48 51 54
13C Chemical shift (ppm)
29-Me
C29
1.60 1.45 1.30 1.15 1.00 0.85 0.70 0.55
1H Chemical shift (ppm)
-3 1 5 9 13 17 21
13C Chemical shift (ppm)

C

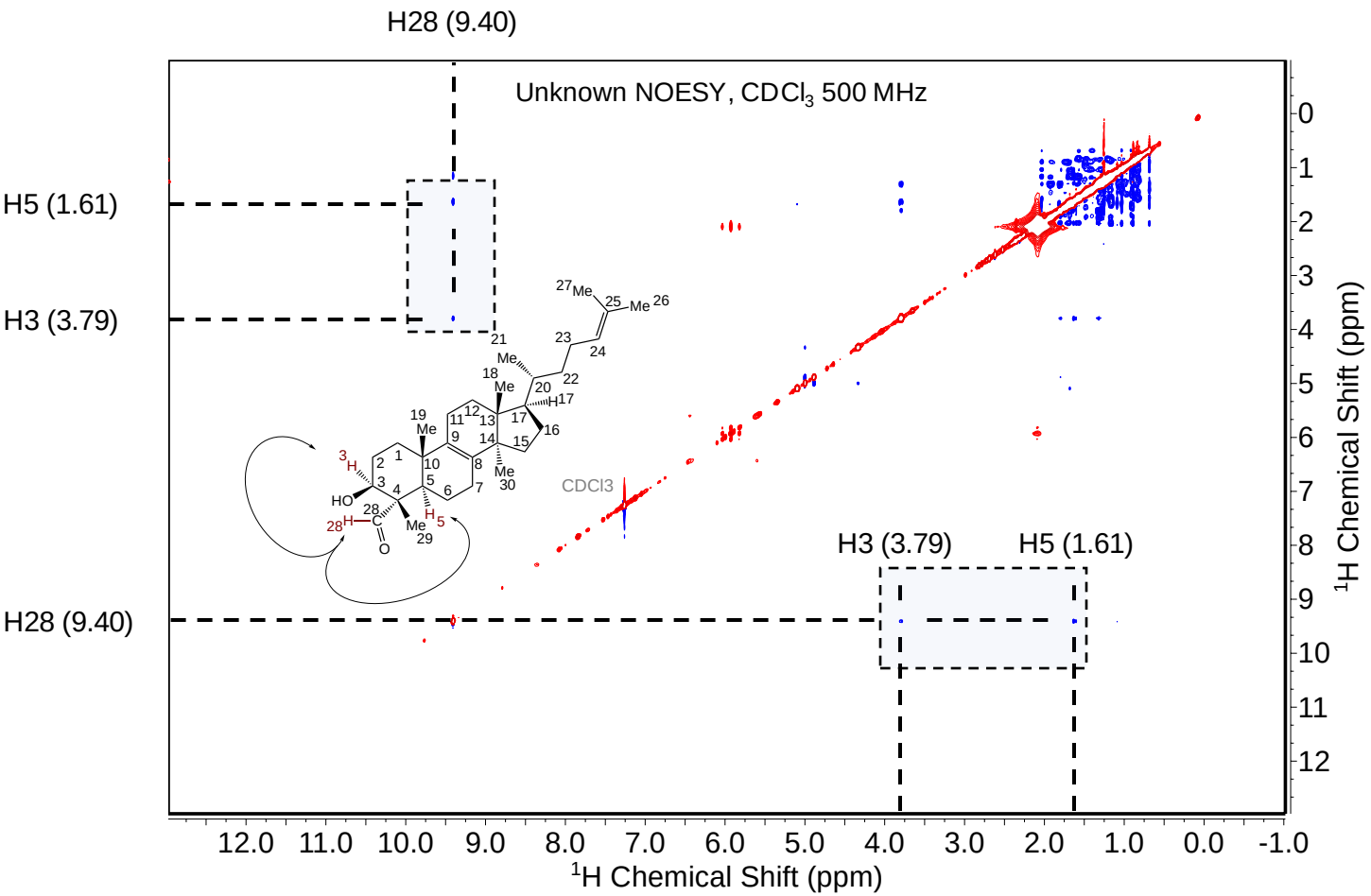
H28 (9.40)
Unknown NOESY, CDCl3 500 MHz
H5 (1.61)
H3 (3.79)
H28 (9.40)
H3 (3.79)
H5 (1.61)
CDCl3
1H Chemical Shift (ppm)
1H Chemical Shift (ppm)

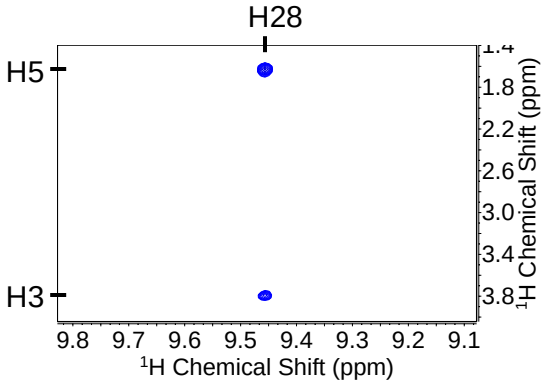
H28
H5
H3
1H Chemical Shift (ppm)
1H Chemical Shift (ppm)

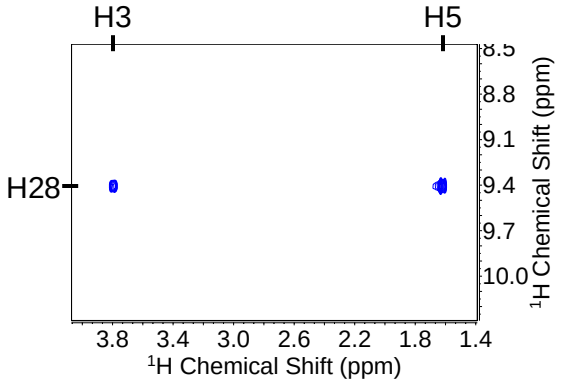
H3
H5
H28
1H Chemical Shift (ppm)
1H Chemical Shift (ppm)

Supplementary Fig. 6. 2D NMR spectra of the purified metabolite (unknown) of lanosterol from incubations with CYP5122A1. (A) HMBC correlations of carbons C28 (aldehyde) and C29 (C4 methyl) with nearby protons H3, H5, H28 (aldehyde), and/or H29 (C4 methyl) and HMBC correlations of the olefinic carbons (C8-9 and C24-25) with nearby protons in the methyl groups. (B) HSQC correlations of carbon C28 and proton H28 in the aldehyde group and carbons C3, C5 and C29 with directly connected protons H3, H5 and H29-Me, respectively. (C) NOESY, through space interactions of the proton H28 (aldehyde) with nearby protons H3 and H5.

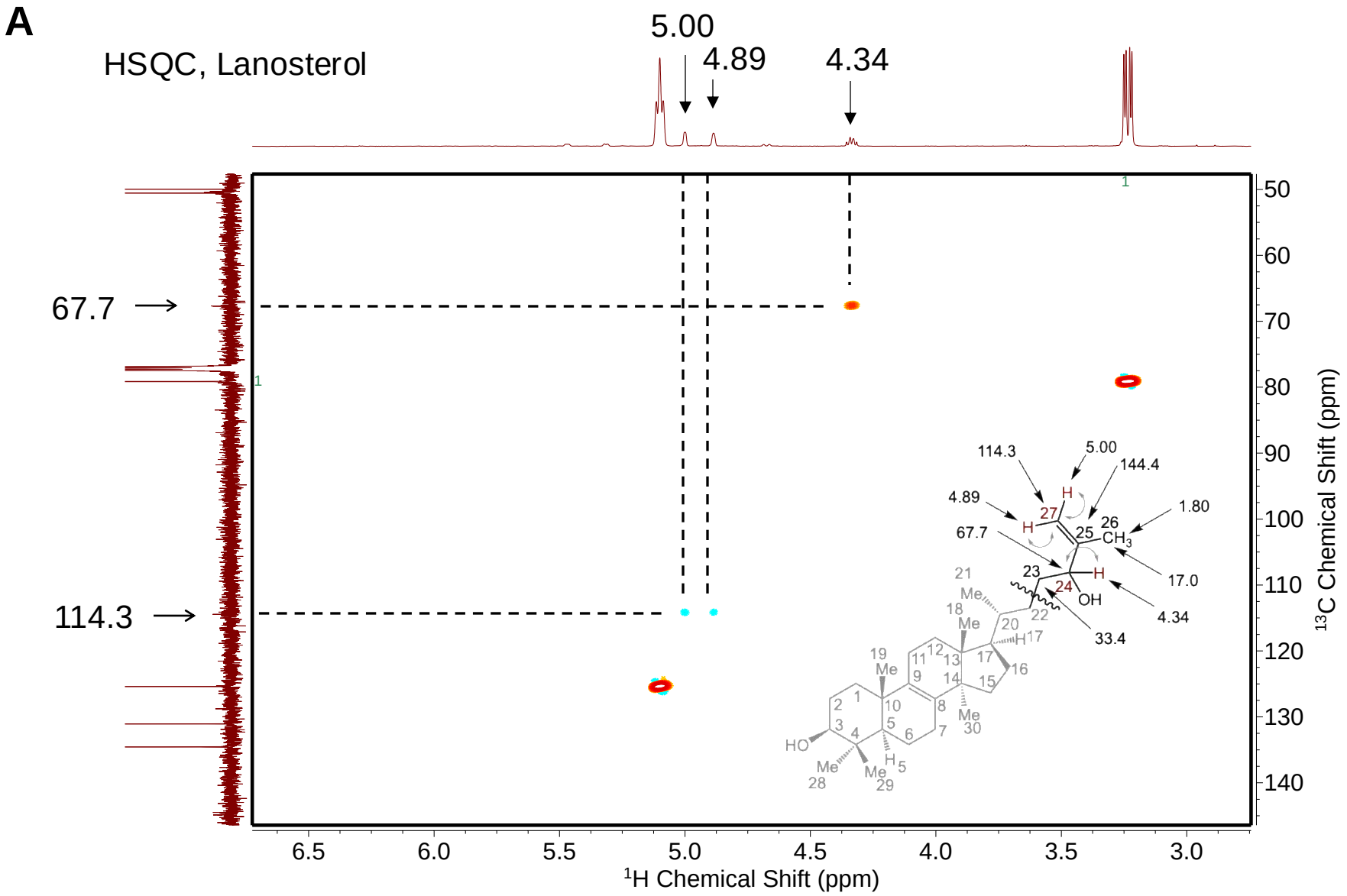
A
HSQC, Lanosterol
5.00
4.89
4.34
67.7
114.3
6.5
6.0
5.5
5.0
4.5
4.0
3.5
3.0
^{1}H Chemical Shift (ppm)
50
60
70
80
90
100
110
120
130
140
^{13}C Chemical Shift (ppm)
114.3
5.00
144.4
4.89
1.80
67.7
17.0
4.34
33.4
Me
HO
OH
CH$_3$

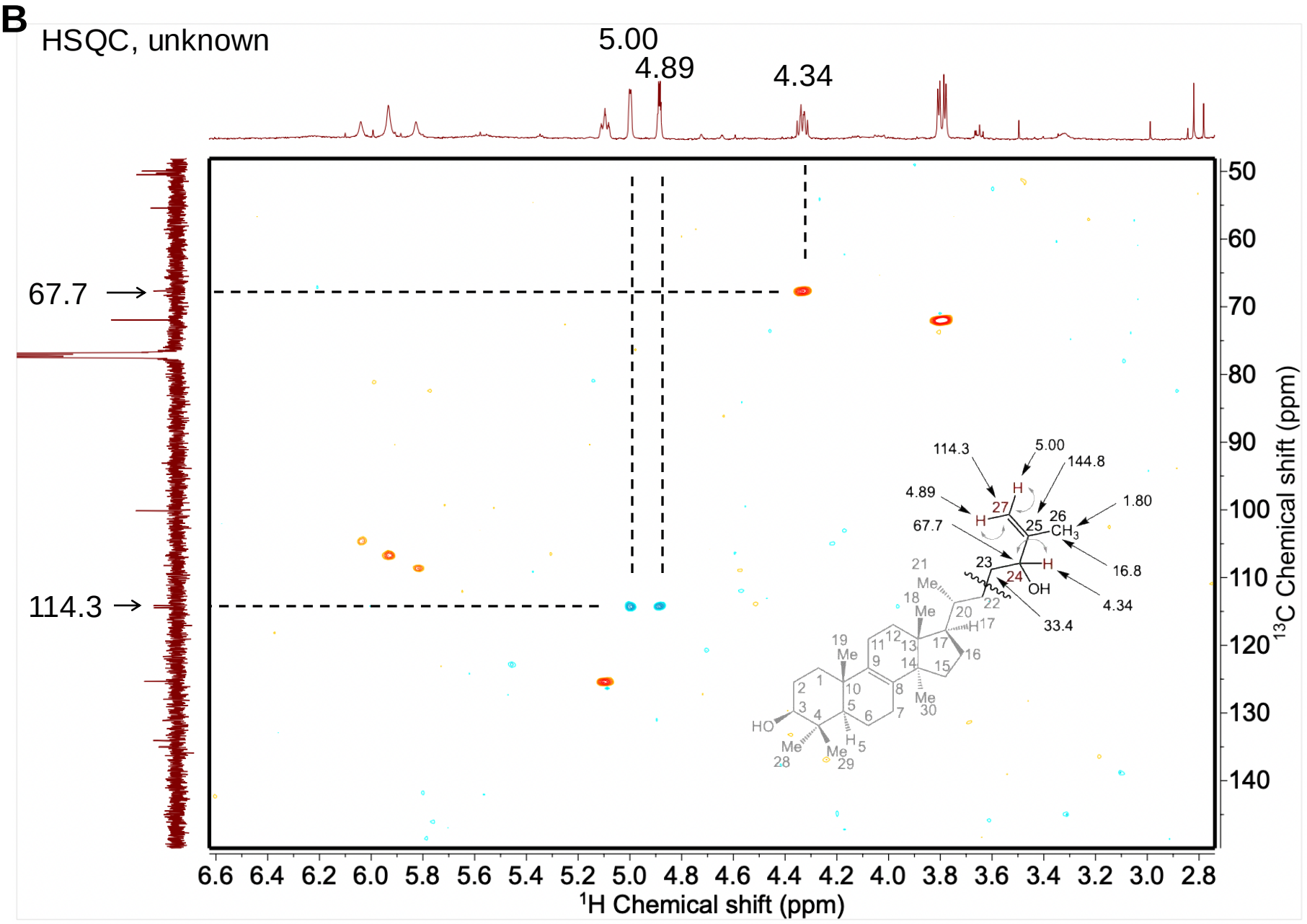
B
HSQC, unknown
5.00
4.89
4.34
67.7
114.3
6.6 6.4 6.2 6.0 5.8 5.6 5.4 5.2 5.0 4.8 4.6 4.4 4.2 4.0 3.8 3.6 3.4 3.2 3.0 2.8
^{1}H Chemical shift (ppm)
50 60 70 80 90 100 110 120 130 140
^{13}C Chemical shift (ppm)
114.3
5.00
144.8
4.89
1.80
67.7
16.8
4.34
33.4
Me
HO
OH
H
CH$_3$

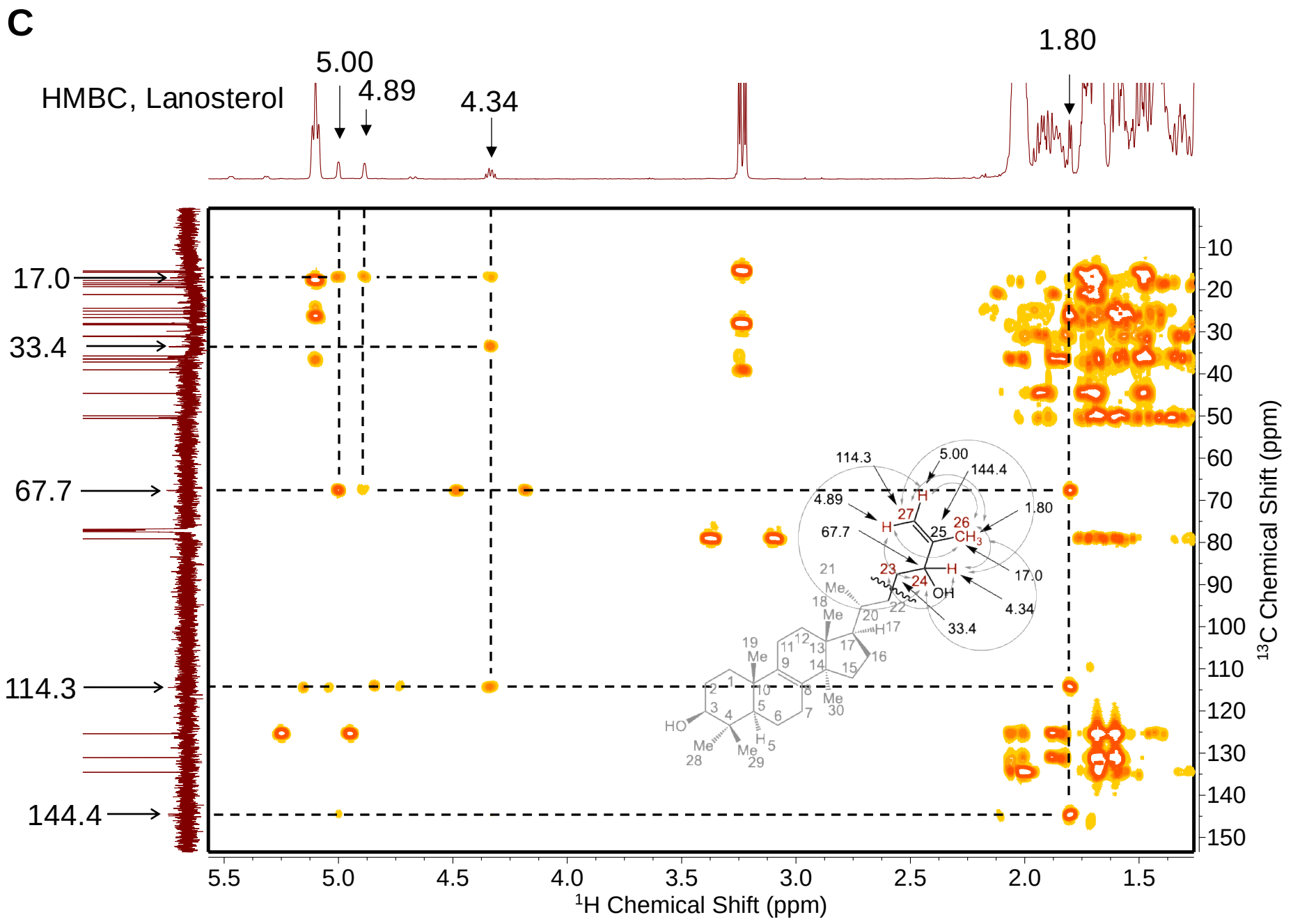
C
HMBC, Lanosterol
5.00
4.89
4.34
1.80
17.0
33.4
67.7
114.3
144.4
5.5
5.0
4.5
4.0
3.5
3.0
2.5
2.0
1.5
^{1}H Chemical Shift (ppm)
^{13}C Chemical Shift (ppm)
10
20
30
40
50
60
70
80
90
100
110
120
130
140
150
114.3
5.00
144.4
4.89
1.80
67.7
17.0
4.34
33.4
HO
Me
OH

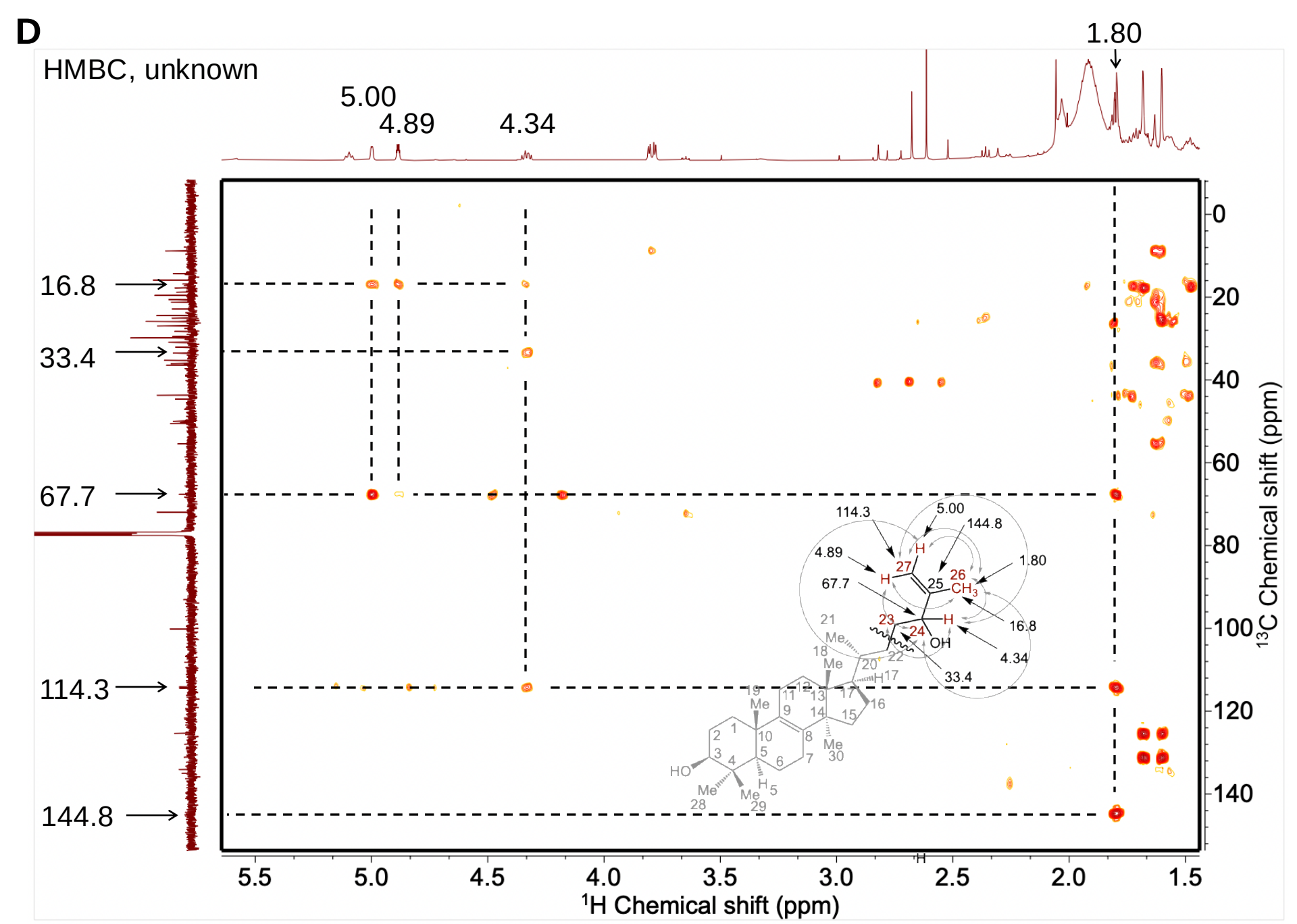
D
HMBC, unknown
1.80
5.00
4.89
4.34
16.8
33.4
67.7
114.3
144.8
5.5
5.0
4.5
4.0
3.5
3.0
2.5
2.0
1.5
^{1}H Chemical shift (ppm)
0
20
40
60
80
100
120
140
^{13}C Chemical shift (ppm)
114.3
5.00
144.8
4.89
1.80
67.7
16.8
4.34
33.4
OH
Me
HO

Supplementary Fig. 7. 2D NMR signals of an impurity (a sterol side chain oxidation product) present in both (A and C) lanosterol standard and (B and D) the purified unknown sample (aldehyde metabolite) from incubations of lanosterol with CYP5122A1. (A and B) HSQC correlations of olefinic carbon C27 with two protons H27 and secondary alcohol carbon C24 with proton H24 in the side chain of the impurity. (C and D) HMBC correlations of olefinic carbon C27 with nearby protons H26 and H24, secondary alcohol carbon C24 with protons H26, H27, carbon C23 with proton H24, and methyl carbon C26 with olefinic protons H27 and proton H24.

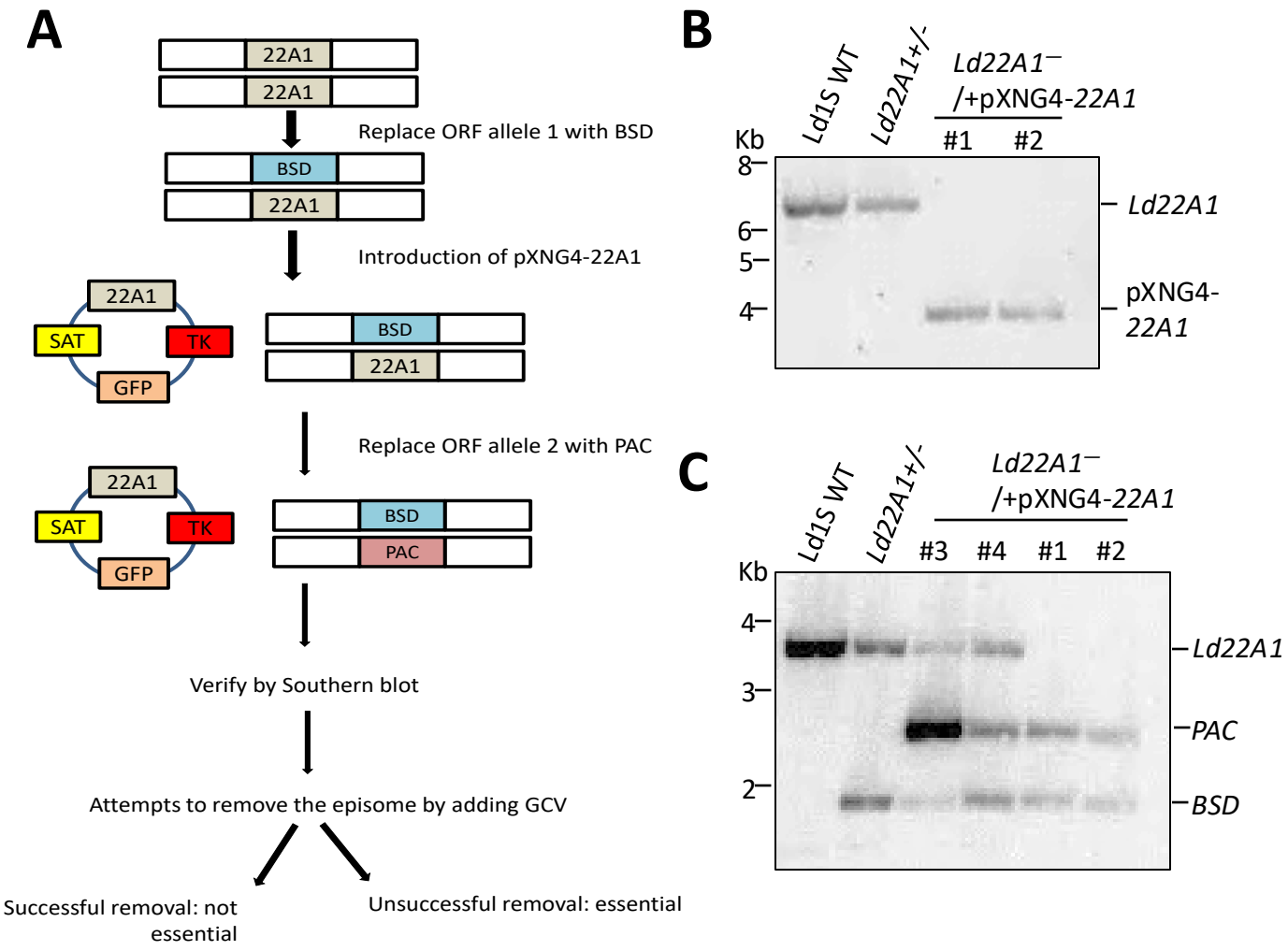

Supplementary Fig. 8. Genetic manipulation of *CYP5122A1* (A) Scheme of assessing the *CYP5122A1* essentiality using a complementing episome-assisted knockout approach coupled with negative selection. Southern blot was processed with genomic DNA from Ld1s WT, Ld22A1$^{+/-}$ and Ld22A1^{-}/+pXNG4-Ld22A1 using radiolabeled *CYP5122A1* ORF probe (B) and 5'-flanking region probe (C). Bands related to Ld22A1, pXNG-Lm22A1, Ld22A1, pXNG-Ld22A1 and antibiotic-resistant genes (BSD/PAC) are indicated. As shown in (C), clone #1-2 were chromosomal-null (Ld22A1^{-}/+pXNG4-Ld22A1) whereas clone #3-4 still contained endogenous *CYP5122A1.*

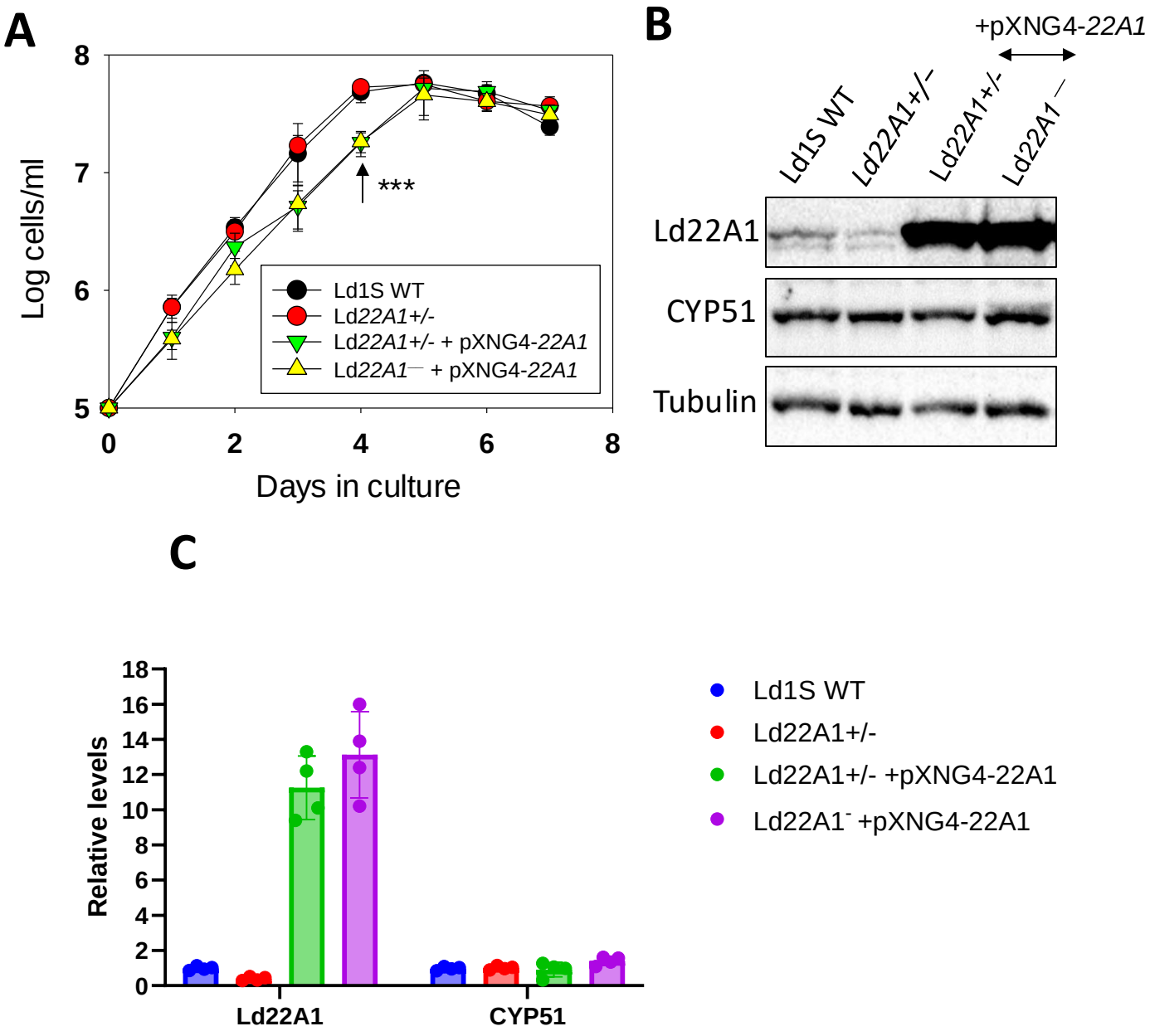

Supplementary Fig. 9. Protein expression levels of CYP51 and CYP5122A1. (A) Log phase promastigotes were inoculated in complete M199 medium and incubated at 27 °C. Culture densities were determined daily. (B) Whole cell lysates from log phase promastigotes were analyzed by western blot using anti-LdCYP5122A1, anti-LdCYP51 or anti-α-tubulin antibodies. (C) Relative abundances of LdCyp5122A1 and CYP51 were quantified using αtubulin as the loading control. Bars and error bars represent the means and standard deviations from three experiments. Two-tailed ANOVA without adjustment (**: $p < 0.01$, ***: $p < 0.001$). Source data are provided as a Source Data file.

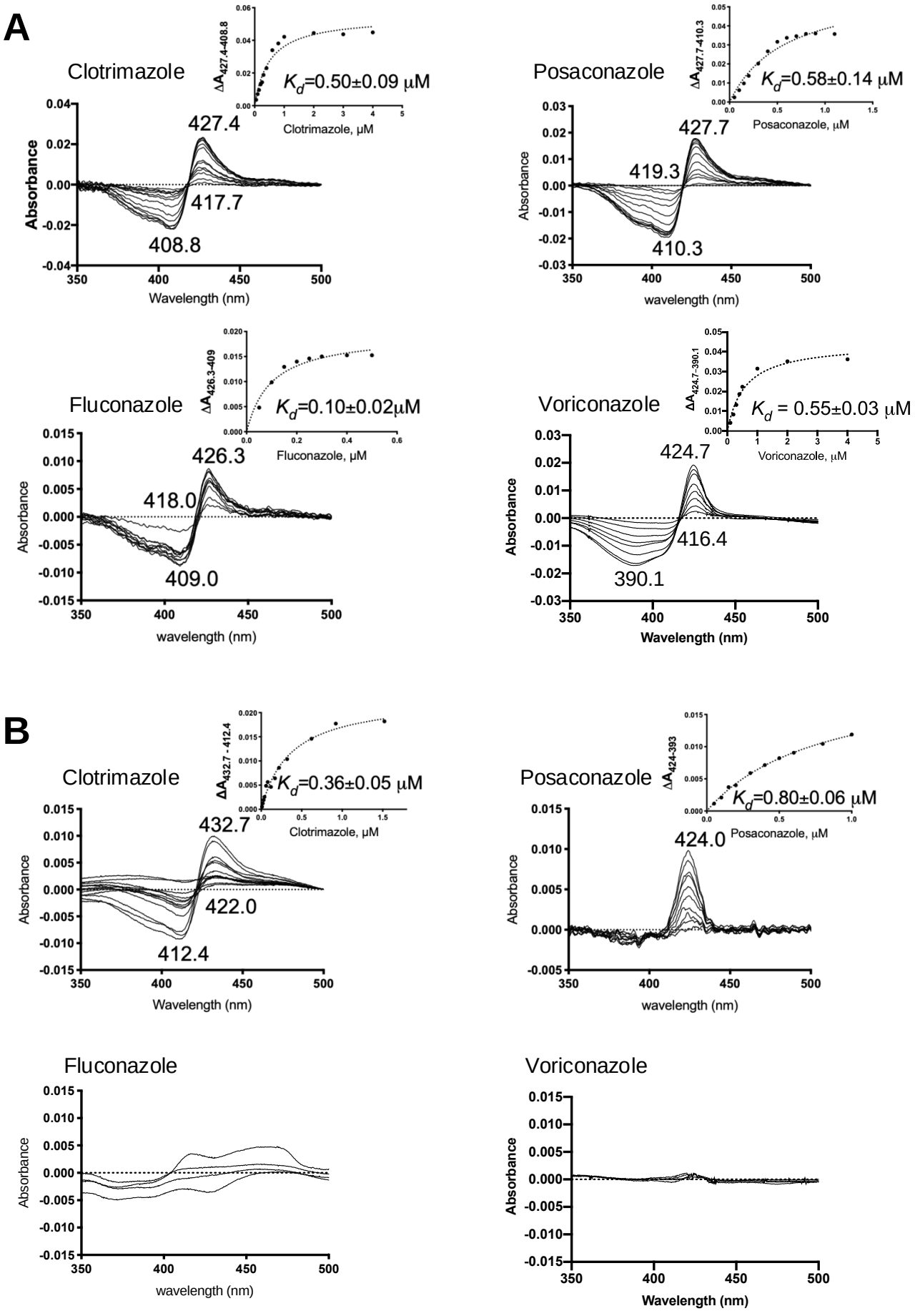
A
Clotrimazole
K_d=0.50±0.09 μM
Clotrimazole, μM
427.4
417.7
408.8
Absorbance
Wavelength (nm)
Posaconazole
K_d=0.58±0.14 μM
Posaconazole, μM
427.7
419.3
410.3
wavelength (nm)
Fluconazole
K_d=0.10±0.02μM
Fluconazole, μM
426.3
418.0
409.0
wavelength (nm)
Voriconazole
K_d = 0.55±0.03 μM
Voriconazole, μM
424.7
416.4
390.1
Wavelength (nm)
B
Clotrimazole
K_d=0.36±0.05 μM
Clotrimazole, μM
432.7
422.0
412.4
Wavelength (nm)
Posaconazole
K_d=0.80±0.06 μM
Posaconazole, μM
424.0
wavelength (nm)
Fluconazole
wavelength (nm)
Voriconazole
Wavelength (nm)

Supplementary Fig. 10. Binding spectra of antifungal azoles with CYP51 (A) and CYP5122A1 (B). Purified recombinant CYPs (in the oxidized ferric form) were incubated with an increasing amount of sterol ligands and difference spectra were recorded over a reference sample that only contained protein and buffer. Dissociation constant (K_d) was derived by fitting the equation $\Delta A = \Delta A_{max}[L]/(K_d + [L])$ to the peak-to-trough absorbance difference (ΔA) versus the ligand concentration ([L]) curve, where ΔA_{max} is the maximal amplitude of the spectral response.

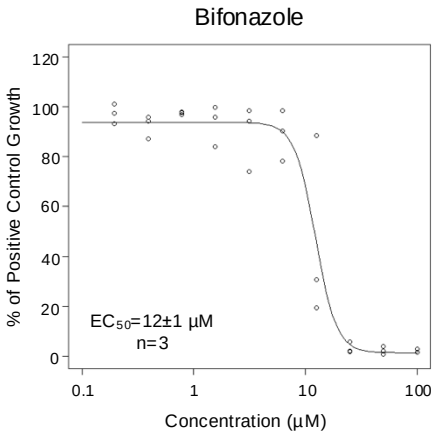
Bifonazole
% of Positive Control Growth
Concentration (µM)
EC50=12±1 µM
n=3

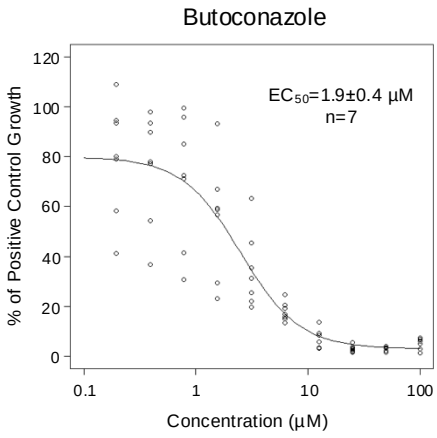
Butoconazole
% of Positive Control Growth
Concentration (µM)
EC50=1.9±0.4 µM
n=7

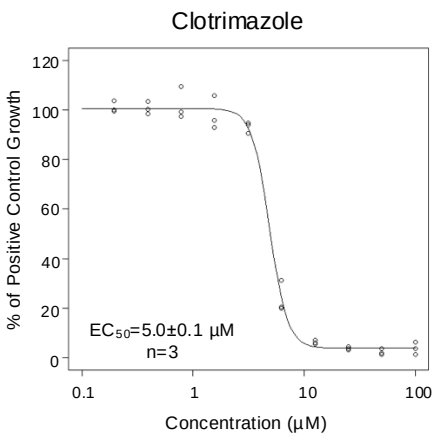
Clotrimazole
% of Positive Control Growth
Concentration (µM)
EC50=5.0±0.1 µM
n=3

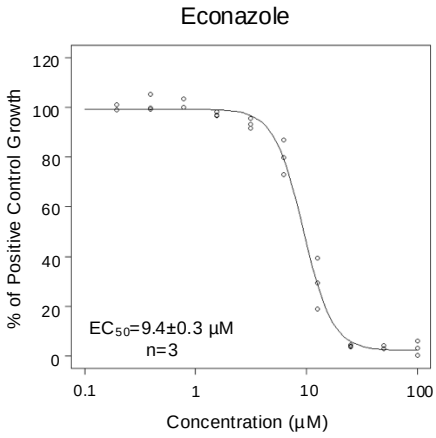
Econazole
% of Positive Control Growth
Concentration (µM)
EC50=9.4±0.3 µM
n=3

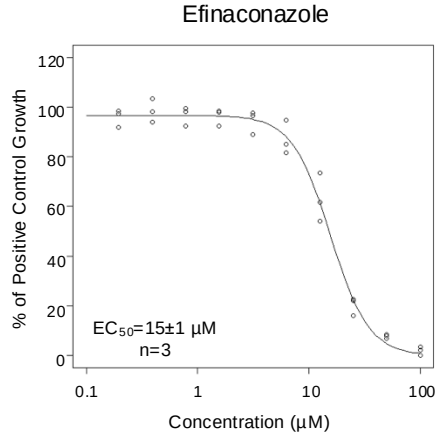
Efinaconazole
% of Positive Control Growth
Concentration (µM)
EC50=15±1 µM
n=3

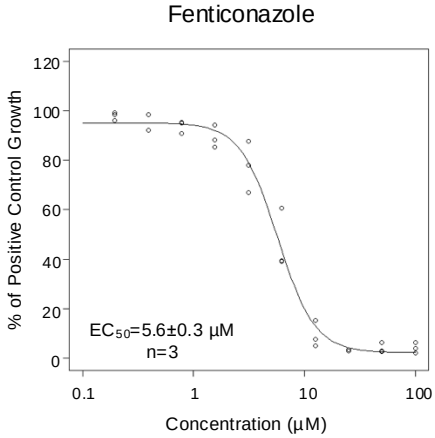
Fenticonazole
% of Positive Control Growth
Concentration (µM)
EC50=5.6±0.3 µM
n=3

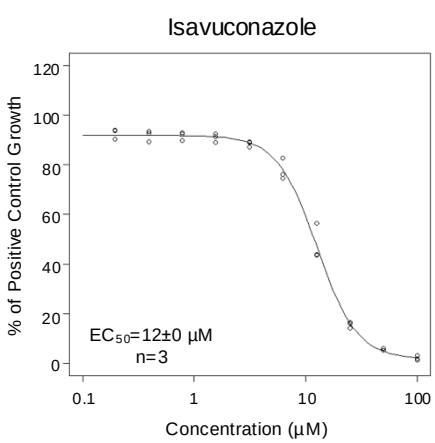
Isavuconazole
% of Positive Control Growth
Concentration (µM)
EC50=12±0 µM
n=3

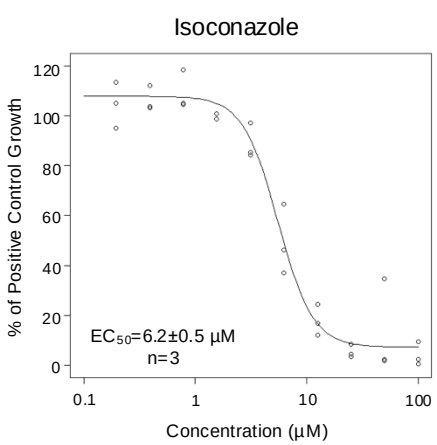
Isoconazole
% of Positive Control Growth
Concentration (µM)
EC50=6.2±0.5 µM
n=3

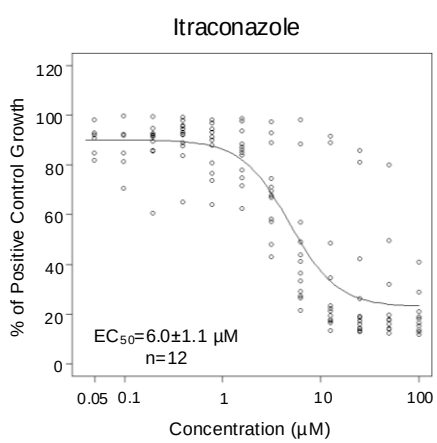
Itraconazole
% of Positive Control Growth
Concentration (µM)
EC50=6.0±1.1 µM
n=12

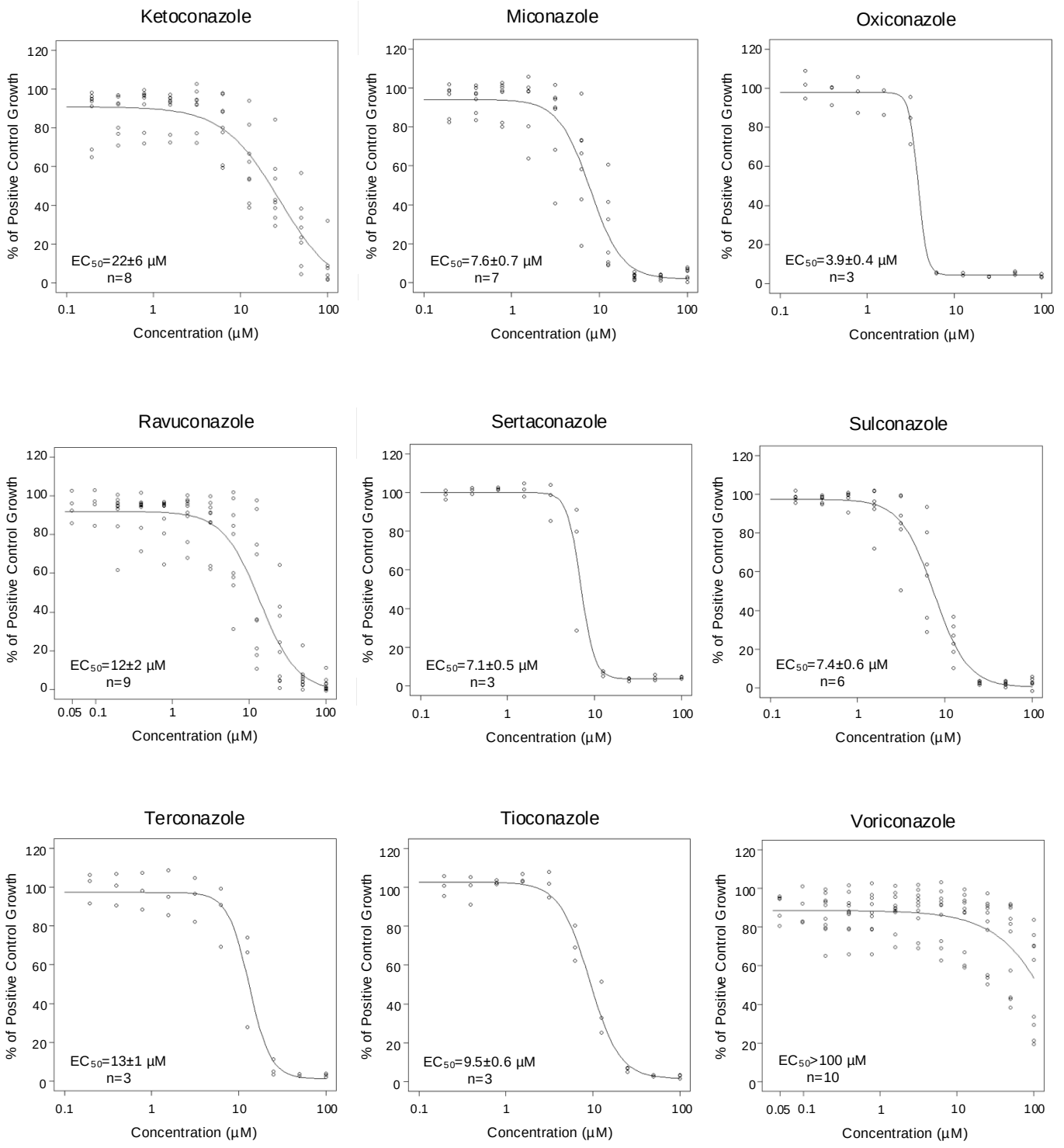

Supplementary Fig. 11. Effect of azole drugs on the proliferation of *L. donovani* LV82 promastigotes. Promastigotes were incubated with serial dilutions of azole drugs and their growth was assessed as described in the Materials and Methods section. Average absolute EC_{50} values along with the standard error obtained by least square fitting are shown on each graph along with the number of independent determinations (n) employed for each azole. Source data are provided as a Source Data file.

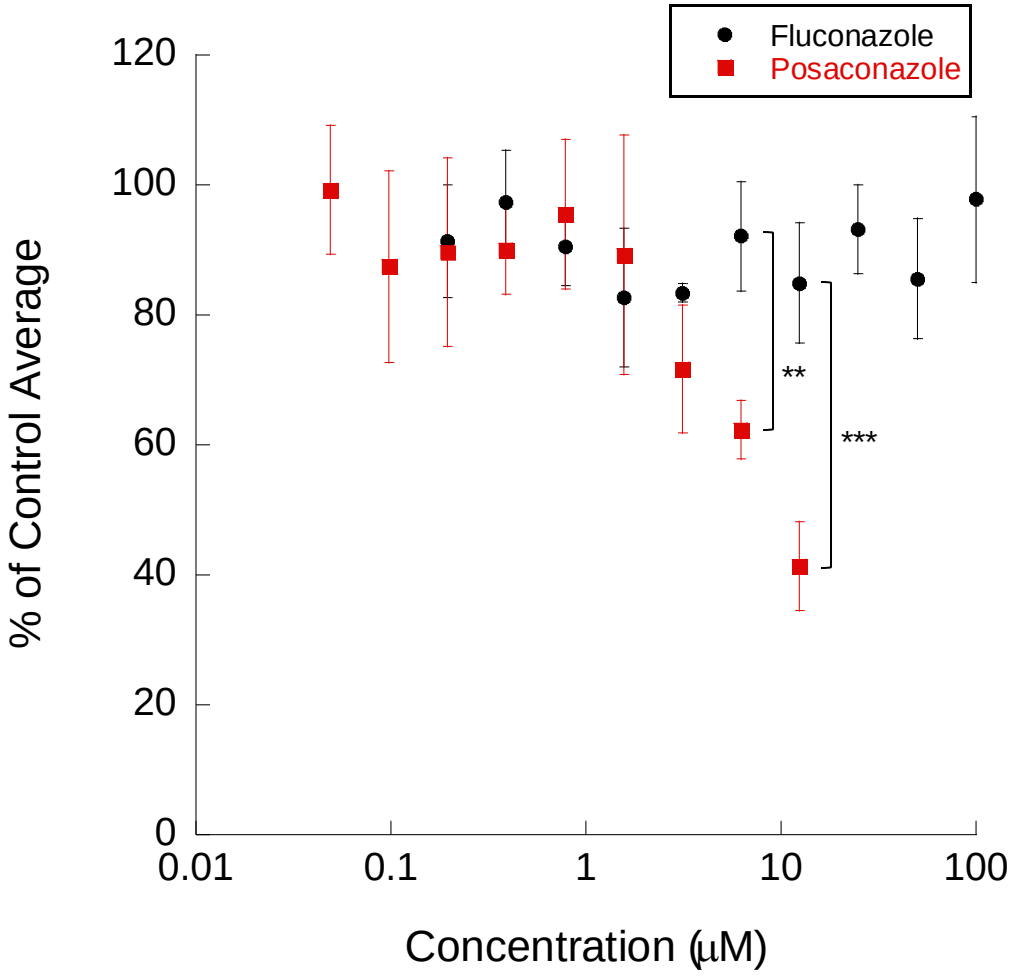

Supplementary Fig. 12. The effect of fluconazole and posaconazole on intracellular *L. donovani*. Peritoneal macrophages were infected with *L. donovani* LV82 parasites for six hours, then were incubated in the presence or absence of serial dilutions of fluconazole or posaconazole for three days as described by Joice et al. (ref. 76). Cells were stained with DAPI and intracellular parasite burden was determined by image analysis as described by Joice et al. (ref. 76). Symbols and error bars represent the means and standard deviations of four independent determinations (**: $p < 0.01$, ***: $p < 0.001$). Note: these data were referred to in the legend of Figure 2 and were plotted in part in Supplementary Figure 3 appearing in ref. 76. Source data are provided as a Source Data file.

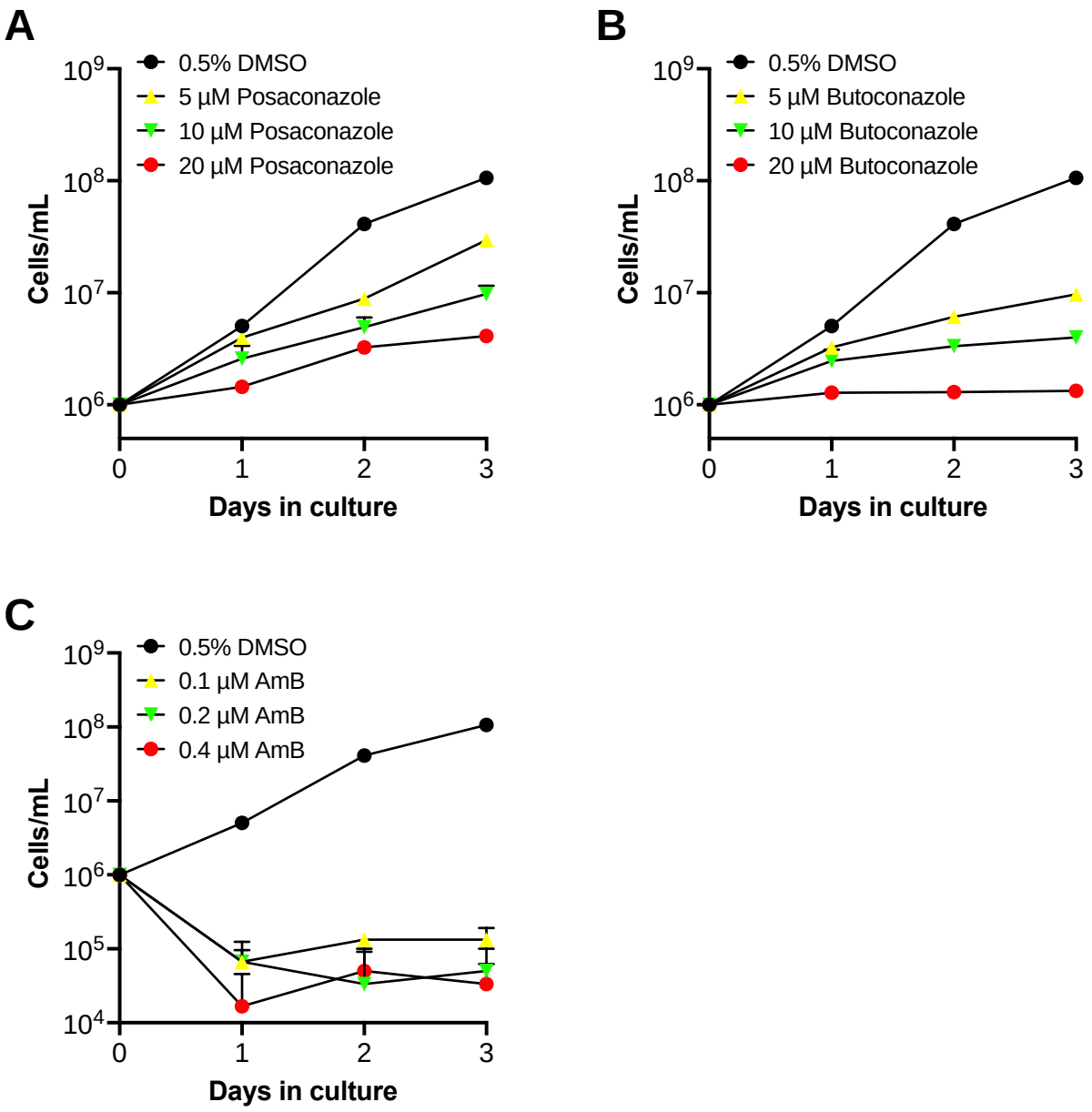

Supplementary Fig. 13. Microscopic counts of *L. donovani* LV82 promastigote cultures exposed to posaconazole, butoconazole, and amphotericin B. Promastigote cultures were incubated with either posaconazole (5, 10, and 20 µM), butoconazole (5, 10, and 20 µM), amphotericin B (0.1, 0.2, and 0.4 µM), or 0.5% DMSO vehicle in 24 well plates at a final volume of 500 µL under the culture conditions outlined in Materials and Methods. Cell counts were performed daily for three days. The average and standard deviation of triplicate measurements are plotted for each condition from the same representative experiment performed on three separate occasions. For clarity, cell densities of cultures maintained in the presence of vehicle or posaconazole are plotted in panel A, cell densities of cultures maintained in the presence of vehicle or butoconazole are plotted in panel B, and cell densities of cultures maintained in the presence of vehicle or amphotericin B are plotted in panel C. Error bars show positive standard deviations because the absence of cells in some samples incubated with 0.2 and 0.4 µM amphotericin B caused the negative error bars to extend below 1 cell/mL. Source data are provided as a Source Data file.

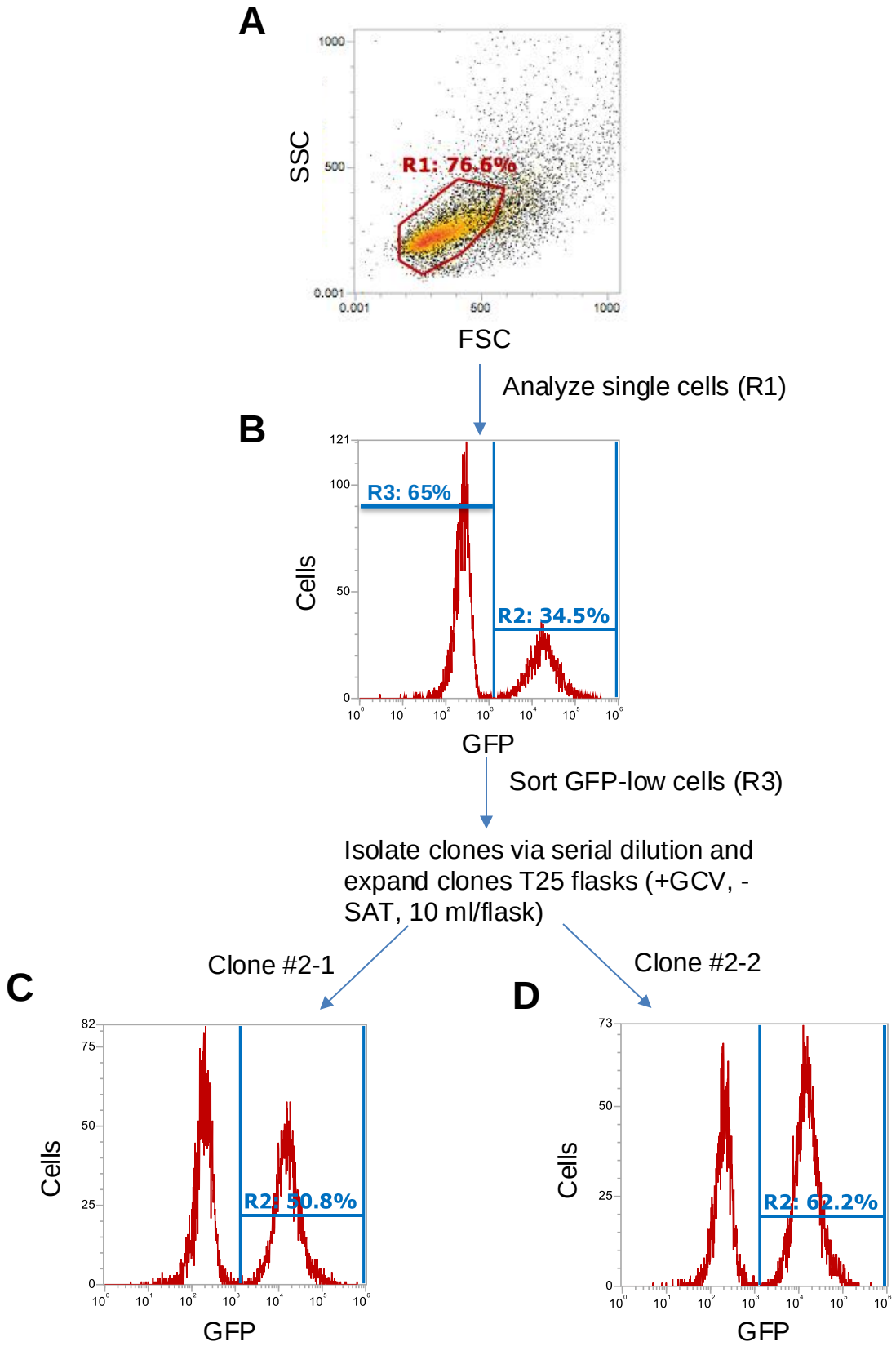

Supplementary Fig. 14. Isolation of GFP-low clones from *Ld22A1*$^{-}$+pXNG4-22A1 by FACS. (A) Single cells (R1) from *Ld22A1*$^{-}$+pXNG4-22A1 #2 grown in the presence of GCV were analyzed for GFP fluorescence (B), and GFP-low cells (R3) were sorted by FACS. Clones were then isolated via serial dilution followed by proliferation in the presence of GCV and absence of SAT. GFP fluorescence for clone #2-1 (C) and #2-2 (D) was analyzed by flow cytometry. Note: B, C and D in this figure are equivalent to Figure 5D, E, and F, respectively.

Supplementary Table 1. Vendor and product information of azole antifungal drugs used in the study.

Chemical Name	Company/Source	Cat. no.	Lot/batch no.
Bifonazole	Alfa Aesar	J63253	I30Z073
Butoconazole nitrate	TCI	B4801	L45WJ-IQ
Clotrimazole	FrontierScientific	496300	L520P36
Econazole	Acros organics	458630050	27220-47-9
Efinaconazole	Sigma	SML1244	046M4752V
Fenticonazole nitrate	TCI	F1008	EFU8K-QC
Fluconazole	Cayman Chem	11594	0449945-13
Isavuconazole	ACHEMBLOCK	M15424	11061
Isoconazole nitrate	Acros organics	458640010	A0362537
Itraconazole	Acros organics	452870050	A0341356
Ketoconazole	TCI America	K00451G	VRTIO-AJ
Miconazole	Alfa Aesar	J60872	M23D029
Oxiconazole nitrate	Sigma	SML1474-10mg	016M4718V
Posaconazole	Carbosynth	FP27107	FP271071401 and 0000029291
Ravuconazole	Sigma	SML1216	055M4724V
Sertaconazole nitrate	eMolecules	QA-5480	A43413
Sulconazole nitrate	Selleckchem	S4120	1
Terconazole	sigma	32355	BCBS8877V
Tioconazole	Alfa Aesar	J60459	Q20E005
Voriconazole	TCI America	V0116	RVK6H-QO

Supplementary Table 2 : Selected ^{1}H and ^{13}C NMR data for lanosterol and the unknown.

Structural Position	^{1}H (ppm)		^{13}C (ppm)	
	Lanosterol	**Unknown**	**Lanosterol**	**Unknown**
18-methyl	0.69	0.68	15.9	15.9
19-methyl	0.98	1.03	19.3	19.6
21-methyl	0.91 (d, J = 6.4 Hz)	0.91 (d, J = 6.4 Hz)	18.8	18.8
26-methyl	1.68	1.68	25.9	25.9
27-methyl	1.60	1.60	17.8	17.8
28-methyl	1.00	_	28.1	_
29-methyl	0.81	1.09	15.6	8.8
30-methyl	0.87	0.88	24.4	24.5
28-aldehyde	_	9.40	_	207.2
-C_3-H_3	3.24 (dd, J = 4.6 Hz, 11.7 Hz)	3.79 (dd, J = 4.1 Hz, 11.5 Hz)	79.1	71.9
-C_4 (quaternary)	_	_	39.0	55.4
-C_5-H_5	1.04	1.61	50.5	43.7
-C_8	_	_	134.5	135.0
-C_9	_	_	134.6	134.1
-C_{24}-H_{24}	5.10 (t, J = 6.6 Hz)	5.10 (t, J = 6.4 Hz)	125.4	125.3
-C_{25}	_	_	131.0	131.2

Supplementary Table 3: Selected ^{1}H and ^{13}C NMR data for an impurity molecule present in both lanosterol standard and the unknown sample. (Proposed side chain structure of the impurity is shown in Supplementary Fig. 7)

Structural Position	^{1}H (ppm)		^{13}C (ppm)	
	Lanosterol	**Unknown**	**Lanosterol**	**Unknown**
23 or other methylene	Unassigned	Unassigned	33.4	33.4
24-CH(OH)	4.34 (q, J = 6.3 Hz)	4.34 (q, J = 6.4 Hz)	67.7	67.7
25-alkene	-	-	144.4	144.8
26-methyl	1.80	1.80	17.0	16.8
27-alkene	4.89 and 5.00	4.89 and 5.00	114.3	114.3

Supplementary Table 4. Primer sequences and purposes

Descriptive name	Purpose	Sequence (5' to 3')
28S rRNA forward	To amplify part of 28S rRNA gene in qPCR (forward primer)	AAGATGGACCGGCCTCTAGT
28S rRNA reverse	To amplify part of 28S rRNA gene in qPCR (reverse primer)	ATCCTTCCCCGCTCCAGTAT
Ld22A1 ORF-F	To amplify the ORF of Ld 22A1 (forward primer)	ATA GTA ggatcc ACC ATG GCC GCG AAC GCG CTT C
Ld22A1 ORF-R	To amplify the ORF of Ld 22A1 (reverse primer)	GCG CT ggatcc TTA CAT GAA CAA CTT GTT CGG TGT GCC
Ld22A1-5'FR-F	To amplify the 5'-flanking region of Ld 22A1 (forward primer)	CAT GCT gaattc CTC TCG TTC TCG TTG GAC
Ld22A1-5'FR-R	To amplify the 5'-flanking region of Ld 22A1 (reverse primer)	GTC CCG actagt CTG AGA ACA GTT CAC AAC
Ld22A1-3'FR-F	To amplify the 3'-flanking region of Ld 22A1 (forward primer)	CGG ACG actagt GGC AAG agatct AGC GAA CTG AGA ATG GCC
Ld22A1-3'FR-R	To amplify the 3'-flanking region of Ld 22A1 (reverse primer)	GTC CAG aagctt CCG TAC AGT CCA TTG CCG
F sequencing primer	To sequence the pcWori+ plasmid to verify insert sequence	GATCAGCTTACTCCCCTTCC
R sequencing primer	To sequence the pcWori+ plasmid to verify insert sequence	CGTATCACGAGGCCCTTTC
Internal sequencing primer	To sequence the pcWori+ plasmid to verify insert sequence for TbCPR	GAGCGAATTGGGGGCCCAGCGCTTCTACC

Uncropped gels and blots for Supplementary Figures

Supplementary Fig. 3A

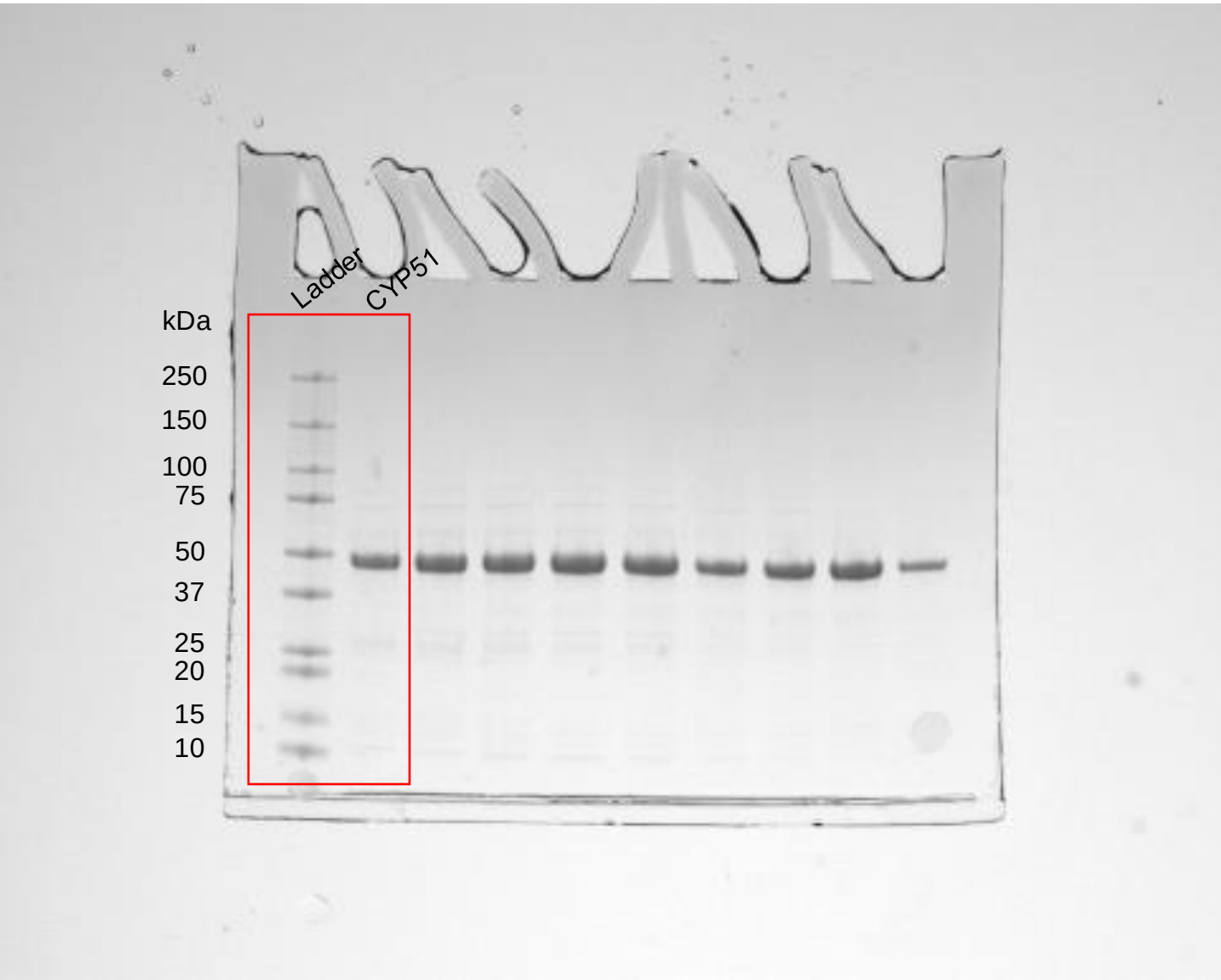

Supplementary Fig. 3B

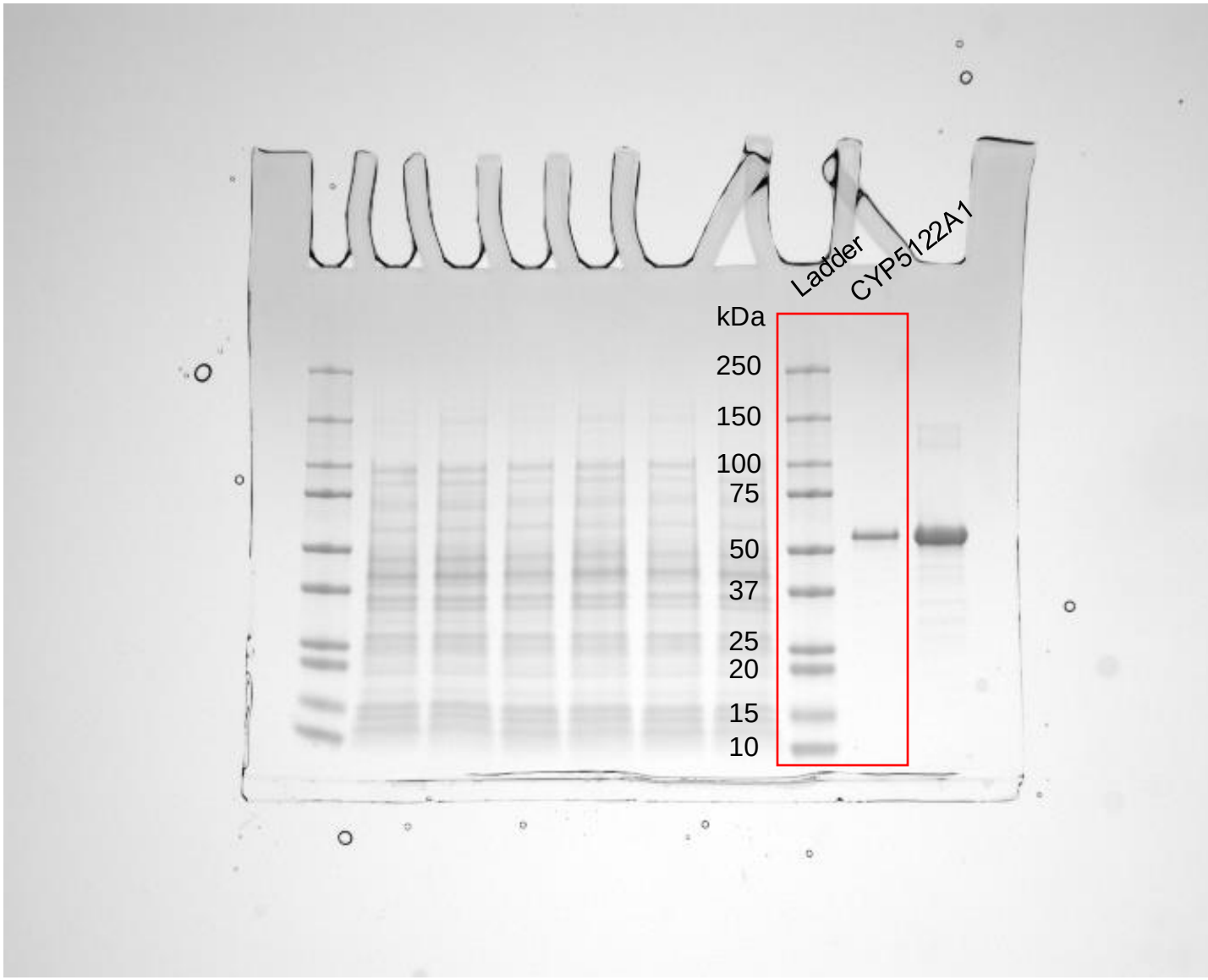

Supplementary Fig. 3C

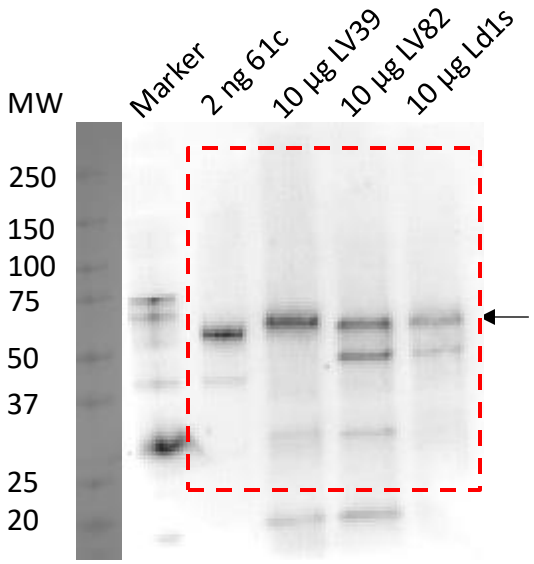

10s exposure

Primary Ab: 1:1000 rat anti-61c serum #1 in 0.1% TBST with 5% milk. Incubate at 4 °C overnight.
Secondary Ab: 1:10,000 goat anti-rat IgG pAb (HRP) (Sigma-Aldrich, AP136P) in 0.1% TBST. Incubate at RT for 2 h.

Supplementary Fig. 8B

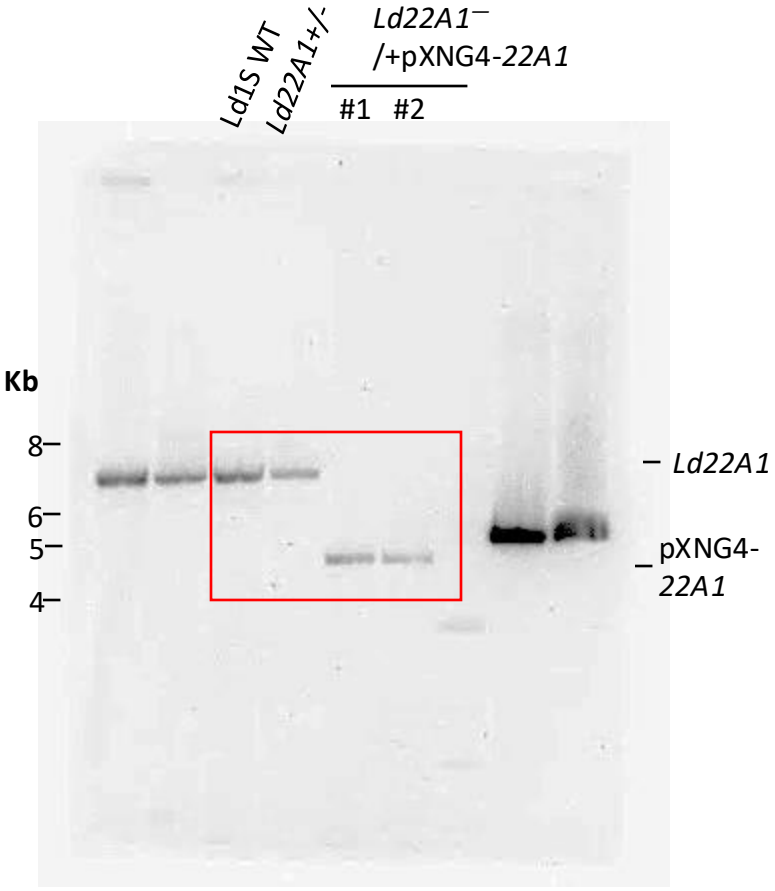

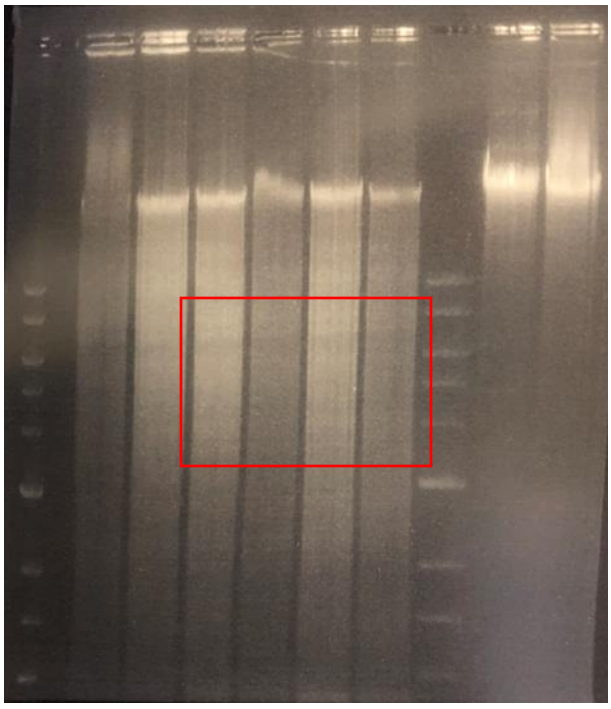

Supplementary Fig. 8C

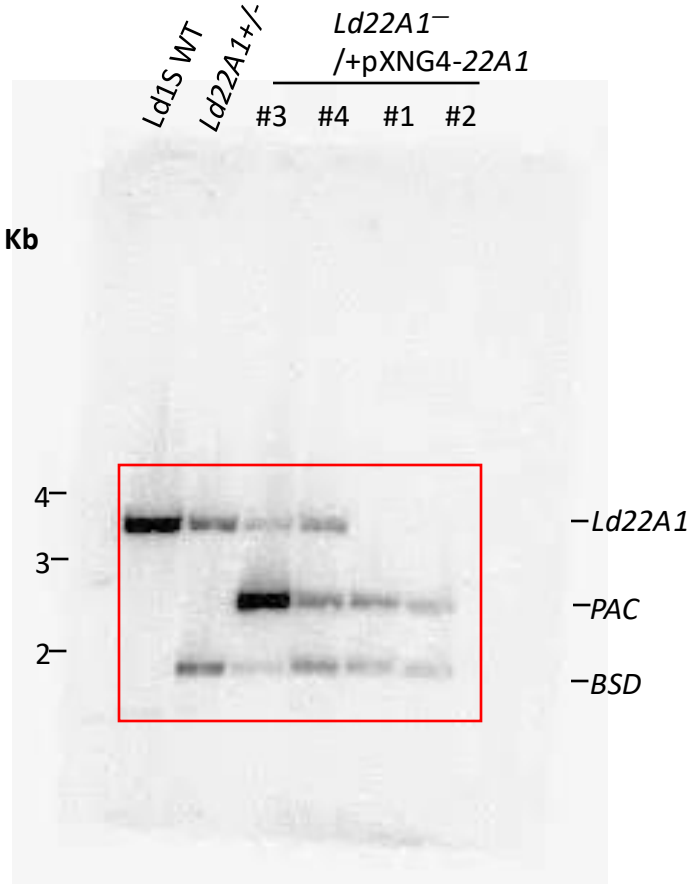

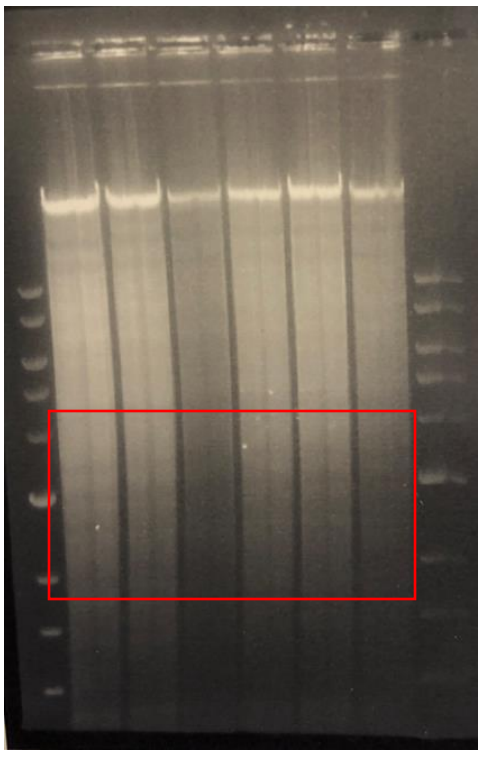

Supplementary Fig. 9B

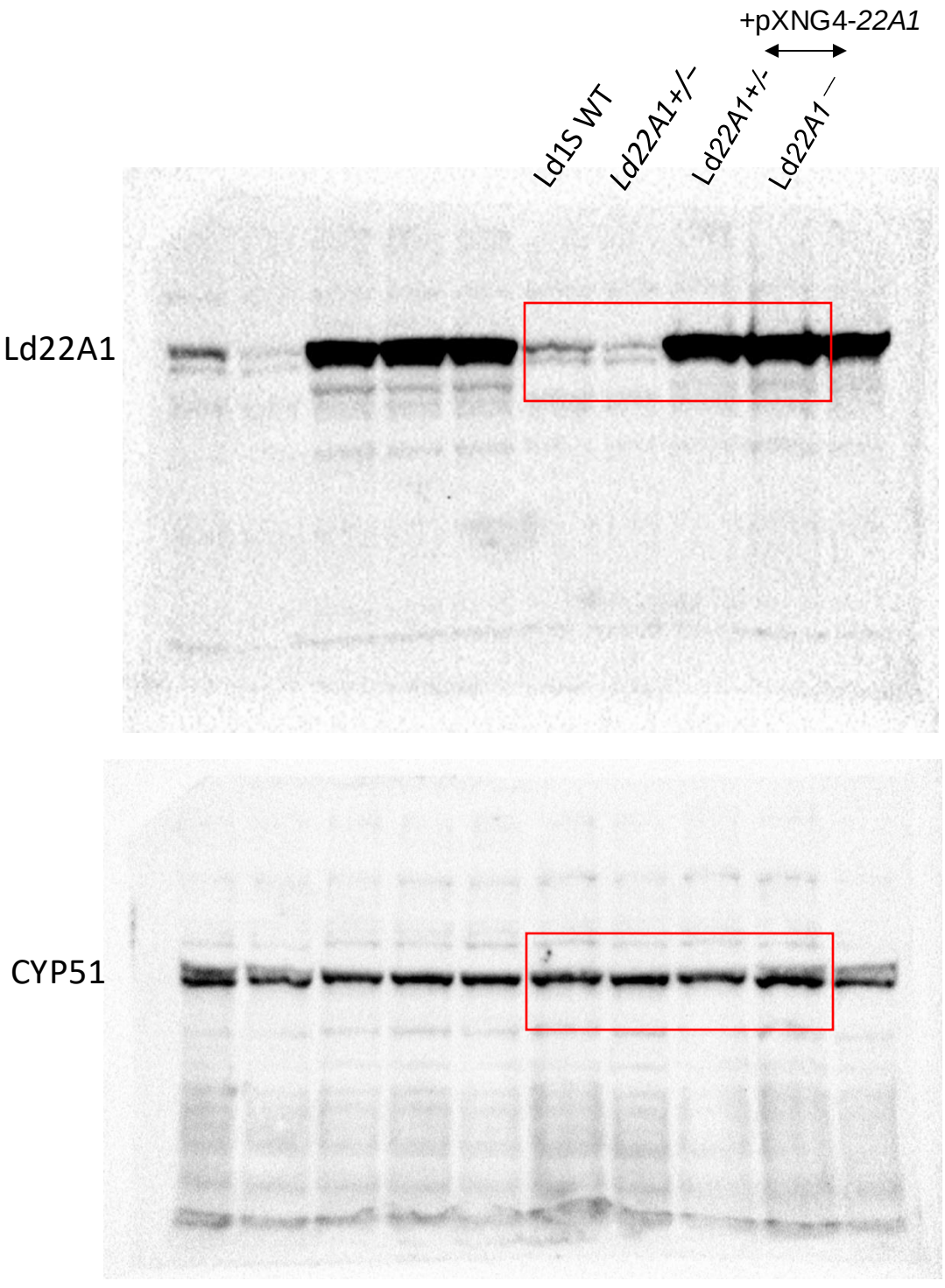

Supplementary Fig. 9B